



# **Suspension design for off-road construction machines**

**Adam Rehnberg**

**Doctoral Thesis**

**TRITA-AVE 2011:39  
ISSN 1651-7660  
ISBN 978-91-7501-040-3**

---

<b>Postal address</b>	<b>Visiting address</b>	<b>Telephone</b>	<b>Internet</b>
Royal Institute of Technology Vehicle Dynamics SE-100 44 Stockholm	Teknikringen 8 Stockholm	+46 8 790 6000 <b>Telefax</b> +46 8 790 9290	<a href="http://www.ave.kth.se">www.ave.kth.se</a>



# Abstract

Construction machines, also referred to as engineering vehicles or earth movers, are used in a variety of tasks related to infrastructure development and material handling. While modern construction machines represent a high level of sophistication in several areas, their suspension systems are generally rudimentary or even nonexistent. This leads to unacceptably high vibration levels for the operator, particularly when considering front loaders and dump trucks, which regularly traverse longer distances at reasonably high velocities. To meet future demands on operator comfort and high speed capacity, more refined wheel suspensions will have to be developed. The aim of this thesis is therefore to investigate which factors need to be considered in the fundamental design of suspension systems for wheeled construction machines.

The ride dynamics of wheeled construction machines are affected by a number of particular properties specific to this type of vehicle. The pitch inertia is typically high in relation to the mass and wheelbase, which leads to pronounced pitching. The axle loads differ considerably between the loaded and the unloaded condition, necessitating ride height control, and hence the suspension properties may be altered as the vehicle is loaded. Furthermore, the low vertical stiffness of off-road tyres means that changes in the tyre properties will have a large impact on the dynamics of the suspended mass. The impact of these factors has been investigated using analytical models and parameters for a typical wheel loader. Multibody dynamic simulations have also been used to study the effects of suspended axles on the vehicle ride vibrations in more detail. The simulation model has also been compared to measurements performed on a prototype wheel loader with suspended axles.

For reasons of manoeuvrability and robustness, many construction machines use articulated frame steering. The dynamic behaviour of articulated vehicles has therefore been examined here, focusing on lateral instabilities in the form of “snaking” and “folding”. A multibody dynamics model has been used to investigate how suspended axles influence the snaking stability of an articulated wheel loader. A remote-controlled, articulated test vehicle in model-scale has also been developed to enable safe and inexpensive practical experiments. The test vehicle is used to study the influence of several vehicle parameters on snaking stability, including suspension, drive configuration and mass distribution. Comparisons are also made with predictions using a simplified linear model.

Off-road tyres represent a further complication of construction machine dynamics, since the tyres’ behaviour is typically highly nonlinear and difficult to evaluate in testing due to the size of the tyres. A rolling test rig for large tyres has here been evaluated, showing that the test rig is capable of producing useful data for validating tyre simulation models of varying complexity.

The theoretical and experimental studies presented in this thesis contribute to the deeper understanding of a number of aspects of the dynamic behaviour of construction machines. This work therefore provides a basis for the continued development of wheel suspensions for such vehicles.



# Sammanfattning

Anläggningsmaskiner, även benämnda entreprenadmaskiner eller arbetsmaskiner, används inom en rad områden relaterade till byggnation eller materialhantering. Moderna anläggningsmaskiner är i flera avseenden sofistikerade system, men har generellt enkla eller obefintliga hjul fjädringar. Detta leder till att föraren utsätts för oacceptabelt höga nivåer av helkropps vibrationer; i synnerhet förare av hjullastare och dumptrar vilka ofta färdas längre sträckor i relativt hög hastighet. För att möta framtida krav på förarkomfort och höga transporthastigheter behöver mer avancerade hjul fjädringar utvecklas. Målet med denna avhandling är därför att undersöka vilka faktorer som behöver beaktas vid utformning av hjul fjädringar för anläggningsmaskiner.

Vertikaldynamiken hos en hjulgående anläggningsmaskin påverkas av ett antal egenskaper som är specifika för fordonstypen. Nicktröghetsmomentet är vanligen högt i förhållande till massan och hjulbasen, vilket leder till en uttalad nicktendens. Axellasterna ändras till stor del då fordonet lastas, vilket innebär att nivåreglering av hjulupphängningen är nödvändig. Detta påverkar fjädringsegenskaperna i lastat tillstånd. Vidare gör däckens låga vertikalstyvhet att ändringar i däckens egenskaper får stor inverkan på den fjädrade massans dynamik. Inverkan av dessa egenskaper har undersökts med hjälp av analytiska modeller och parametrar för en typisk hjullastare. Simuleringar med stelkroppsmodeller har också utnyttjats för att studera i detalj hur fjädrade axlar inverkar på färdvibrationerna. Resultaten från simuleringar har jämförts med provdata från en hjullastarprototyp med fjädrade axlar.

Flera anläggningsmaskiner använder ramstyrning, vilket ger hög manövrerbarhet och robusthet. Det dynamiska beteendet hos ramstyrda fordon har därför undersökts, med fokus på instabila laterala fenomen i form av ”slingring” eller ”vikning”. En dynamisk simuleringsmodell har använts för att undersöka hur fjädrade axlar påverkar den laterala stabiliteten hos en ramstyrd hjullastare. Ett fjärrstyrt provfordon i modellskala har också utvecklats, vilket ger möjlighet till praktiska experiment med låg risknivå och kostnad. Provfordonet har utnyttjats för att studera inverkan av flera fordonsparametrar såsom hjul fjädring, drivlinans egenskaper samt massfördelning. Jämförelser har också gjorts med predikteringar från en förenklad, linjär modell.

Däck för terrängfordon är vanligen starkt olinjära, vilket ytterligare komplicerar anläggningsmaskinens dynamik. På grund av de stora däcksdimensionerna är egenskaperna för däcken dessutom svåra att bestämma experimentellt. En rullande provrigg för stora däck har blivit utvärderad och visar att riggen kan producera användbara mätdata för att validera däckmodeller av varierande komplexitet.

De teoretiska och experimentella studierna som presenteras i denna avhandling bidrar till en ökad förståelse av anläggningsmaskiners dynamik ur ett flertal aspekter. Arbetet utgör därmed en grund för en fortsatt utveckling av fjädringssystem för sådana fordon.

*“To define it rudely but not ineptly, engineering is the art of doing for 10 shillings what any fool can do for a pound.”*

The Duke of Wellington, Arthur Wellesley

# Acknowledgements

This thesis marks the end of my excursion as a doctoral student into the world of heavy vehicle dynamics. I am indebted to a number of persons and organisations that have all made this endeavour possible.

Financing was provided by Volvo Construction Equipment and VINNOVA in the first stage, and in the later phases by the VINN Excellence Centre for ECO<sup>2</sup> Vehicle Design. The support of these partners is gratefully acknowledged.

Many thanks are extended to my main supervisor, Associate Professor Lars Drugge, who has been responsible for the day-to-day supervision and whose brilliance in both academic and technical matters has been absolutely crucial for the success of this thesis. Thanks are also due to my secondary supervisor Professor Annika Stensson, for accepting me as a doctoral student in the first place and for providing enthusiastic assistance along the way.

I am also thankful to everyone at Volvo Construction Equipment who has been actively involved in my research. Firstly, thanks are extended to Professor Jack Samuelsson and Mr Ulf Petersson, for initiating and supervising the project in the early stages. Moreover, many thanks are given to Andreas Nordstrand, Henrik Eriksson, Allan Ericsson, Heikki Illerhag, Patrik Örtenmark, Reza Renderstedt and Johan Ohlsson for helping with practical knowledge about construction machine design and applied dynamic analysis, and also for providing test resources. The input and support from an industrial partner have been invaluable for the quality and applicability of the results, while also providing a much appreciated contact with reality. Doctoral student Kent Cronholm deserves mentioning as well, for helpful information regarding the inner workings of the Volvo CE company and construction machines in general.

Within the Centre for ECO<sup>2</sup> Vehicle Design, I am thankful to the Steering Group of the Suspension Design project for providing valuable advice while at the same time allowing me to pursue my own ideas. Thanks are also extended to the Centre's management for giving me the opportunity to participate in activities arranged for the whole centre and taking place outside my own project, thus widening my perspective on sustainable vehicle design and providing a valuable framework for my research. Thanks are due to my fellow doctoral students within the ECO<sup>2</sup> Centre as well, for letting me become acquainted with their research and for providing a highly enjoyable social dimension to the research work.

Thanks are given to my fellow doctoral students and senior colleagues at the Division of Vehicle Dynamics, for providing a welcoming atmosphere and stimulating discussions about research, teaching and various aspects of vehicle engineering. Thanks are also due to the numerous MSc and BSc students who have been contributing to the project through their thesis work and project assignments, while at the same time allowing me the joy of teaching and mentoring.

Thanks are also extended to the colleagues and management of LUTAB, whose support of and interest in my work have been highly motivating along the course of my research.

Many thanks are extended to Professor Pieter Schalk Els and the Vehicle Dynamics Research Section at the University of Pretoria, South Africa. By allowing me to take part in the tyre measurement project, you provided a much-sought element of international cooperation and experimental work for this thesis. The value of this experience in terms of research quality and personal development cannot be overestimated and I am highly thankful for this opportunity.

Finally, thanks to all of my friends and family for continuous support and motivation throughout the work.

Stockholm, 18 May 2011

Adam Rehnberg

# Appended Papers

This thesis consists of an introductory part and the following five appended papers:

## Paper A

Rehnberg, A., Drugge, L. (2008), *Ride comfort simulation of a wheel loader with suspended axles*, Int. J. Vehicle Systems Modelling and Testing, Vol. 3, No. 3, pp. 168-188.

Rehnberg developed the models, performed the simulations and wrote the paper. Drugge assisted with the simulation parameters, test scenarios and conclusions.

Parts of the results from this study were included in a poster presentation at the 20th Symposium of the International Association for Vehicle System Dynamics (IAVSD), August 13-17, 2007, Berkeley CA, USA.

## Paper B

Rehnberg, A., Drugge, L. (2007), *Pitch comfort optimisation of a front end loader using a hydropneumatic suspension*, SAE Technical Paper 2007-01-4269, SAE 2007 Transactions, Journal of Commercial Vehicles, Section 2, Vol. 116. Presented at the SAE 2007 Commercial Vehicle Engineering Congress and Exhibition, October 31 – November 2, 2007, Rosemont IL, USA.

Rehnberg developed the models, performed the calculations and simulations, and wrote the paper. Drugge provided input on the theory, test scenarios and models.

## Paper C

Rehnberg, A., Drugge, L. (2010), *Influence of tyre properties on the ride dynamics of heavy off-road vehicles*. Paper presented at the joint 9th Asia-Pacific ISTVS Conference and Annual Meeting of Japanese Society for Terramechanics, September 27-30, 2010, Sapporo, Japan.

Rehnberg developed the models, performed the calculations and wrote the paper. Drugge provided feedback on the parameter studies and results analysis.

## Paper D

Rehnberg, A., Drugge, L., Stensson Trigell, A. (2010), *Snaking stability of articulated frame steer vehicles with axle suspension*, Int. J. Heavy Vehicle Systems, Vol. 17, No. 2, pp. 119-138, 2010.

Rehnberg developed the models and evaluation method, performed the simulations and wrote the paper. Drugge assisted with the test scenarios and evaluation criteria. Stensson Trigell assisted with writing the paper.

## Paper E

Rehnberg, A., Edrén, J., Eriksson, M., Drugge, L., Stensson Trigell, A., *Scale model investigation of the snaking and folding stability of an articulated frame steer vehicle*. Article in press, Int. J. Vehicle Systems Modelling and Testing.

Rehnberg conceived the idea, specified the requirements for the test vehicle, performed the theoretical analysis and wrote the paper. Edrén and Eriksson designed and built the test vehicle and performed all the measurements. Drugge assisted with the vehicle design specification, the results analysis and the writing of the paper. Stensson Trigell supervised the work and assisted by proofreading the paper.

The main results of this study were presented orally at Svenska Mekanikdagarna, June 15-17, 2009, Södertälje, Sweden.

# Contents

<b>1. Introduction and background.....</b>	<b>1</b>
1.1 An introduction to construction machines .....	1
1.2 The drive for further evolution .....	2
1.3 Research approach .....	4
1.4 Methods used.....	5
1.5 Outline of this thesis .....	5
<b>2. Ride dynamic aspects .....</b>	<b>7</b>
2.1 Fundamental pitch and bounce dynamics .....	7
2.2 Roll dynamics .....	24
2.3 Higher order dynamics.....	25
<b>3. Lateral dynamics of articulated frame steer vehicles .....</b>	<b>27</b>
3.1 Planar analysis .....	28
3.2 Expanded linear analysis .....	31
3.3 Multibody dynamic simulations .....	31
3.4 Scale model tests.....	34
<b>4. Effects of dynamic properties of large off-road tyres .....</b>	<b>39</b>
4.1 Related work on vertical properties .....	39
4.2 Related work on lateral properties .....	42
4.3 Evaluation of a rolling test rig for large tyres .....	43
<b>5. Multibody dynamics simulation and validation.....</b>	<b>45</b>
5.1 Formalism and analysis modes .....	45
5.2 Model validation.....	46
5.3 Multibody dynamics simulation of a suspended wheel loader .....	48
<b>6. Summary and discussion of appended papers .....</b>	<b>55</b>
<b>7. Scientific contributions.....</b>	<b>59</b>
<b>8. Conclusions and recommendations for future work .....</b>	<b>61</b>
 <b>Appendix 1: Determining characteristics of large tyres by using full vehicle dynamic testing .....</b>	 <b>71</b>



# 1. Introduction and background

## 1.1 An introduction to construction machines

Since the origin of the first steam-powered excavating machines in the 19th century (Gransberg, Popescu and Ryan, 2006), mobile construction machines have been crucial for the development of modern infrastructure. While most early machines were basically modified agricultural tractors, modern construction machines have evolved into purpose-built, integrated vehicles. Some examples of common construction machine types can be seen in figure 1.



Figure 1: Common machine types: wheel loader (a), articulated dump truck and excavator (b), bulldozer (c).

The most elementary task for a construction machine is *earth moving* – excavating and/or moving soil, sand, rock or similar crude material from one location to another. While most machines are designed with this task in mind, construction machines can be found in numerous other roles, such as pallet handling, pipe laying, or any other task that requires a rugged vehicle with high load capacity and off-road capability. Earth moving, as well as many other types of transport tasks performed by construction machines, is usually performed in driving cycles that include loading, transporting and unloading the material. A schematic of an earth-moving cycle, including possible additional tasks, can be seen in figure 2 (Day, 1973). Referring to this definition, the transport capacity of an earth-moving machine can be described by two basic parameters: the amount of material carried per cycle, and the total cycle time.

Increasing the task performance can therefore be accomplished either by increasing the load capacity, or shortening the cycle time.

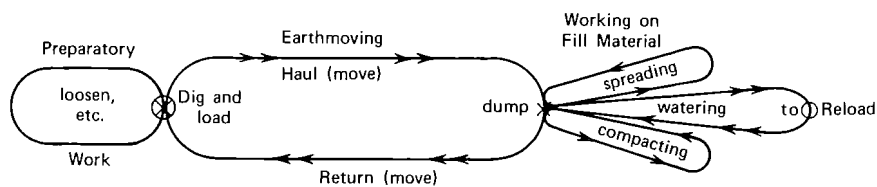


Figure 2: Schematic of an earth-moving cycle (Day, 1973).

Depending on the specifics of the earth-moving operation, various machines may be selected for the task. The research work presented in this thesis focuses on the vehicle dynamic behaviour of the machine, meaning that the relevant parts of the work cycle are the “haul” and “return” phases of figure 2. Thus, the machines of interest are those that travel over reasonably long distances at higher speeds, mainly including front loaders and dump trucks. Excavators, scrapers, bulldozers and similar machines are either used at very low speeds or mainly in a stationary position, meaning that vehicle dynamic behaviour is less relevant to these machine types.

## 1.2 The drive for further evolution

The evolution of construction machines has historically been driven primarily by productivity demands. Therefore, the load capacity is the primary figure of merit, followed by secondary objectives such as tractive performance, reliability, durability and ease of maintenance. Vehicle dynamic qualities such as ride comfort and handling quality have been considered less important, which is reflected in the lack of refined wheel suspensions. Usually construction machines feature at best rudimentary suspension systems, and often rely solely on the tyres to provide vibration isolation and road holding. The vehicle layout may also be less optimal with regard to the ride and handling characteristics, instead being optimised for maximum load capacity and ease of operation.

The lack of refined suspension systems, in combination with the rough surfaces where construction machines operate, generally means that vibration levels in earth-moving machines are high. An example of measured whole-body vibration values in various earth-moving machines is presented in table 1. These measurements have been taken at various Canadian worksites (Cann et al, 2003) and are presented as RMS accelerations, measured and filtered according to the ISO 2631-1 standard (ISO, 1997). The detrimental health effects of whole-body vibrations are well known, including back pain and various internal organ disorders (Bovenzi and Hulshof, 1998), and vibration exposure can therefore be considered a major occupational hazard for earth mover operators.

Table 1: Whole-body vibration levels in typical earth-moving machines (Cann et al, 2003).

<b>Machine type</b>	<b>Mean acceleration [m/s<sup>2</sup>]</b>
Wheel loader	1.16
Dump truck	1.21
Backhoe loader	1.05
Skid steer loader	1.18

In comparison, the European Vibration Directive (European Parliament, 2002) states that vibration values above  $0.5 \text{ m/s}^2$  mandate that the employer must take action to reduce vibration-exposure. Furthermore, the directive states that no operator shall at any time be exposed to vibration levels exceeding  $1.15 \text{ m/s}^2$ . Clearly, a significant improvement in ride comfort is called for if the regulations are to be complied with without major organisational changes.

Whole-body vibrations are only countered to some degree by current technology. Cab and seat suspensions may alleviate vibrations, but they are limited by the short stroke length available and are mainly effective in the vertical direction. It has also been seen that, due to inadequate design, many seats actually amplify vibrations in the critical frequency range, thus aggravating the situation rather than improving it (Donati, 2002). Increased tyre damping could possibly improve vibration isolation in vehicles without suspension, but is generally undesirable due to increased rolling resistance and thermal stress (Lines, Stiles and Whyte, 1995). Moreover, off-road tyre design is generally governed primarily by demands for durability and traction, which limits the possibility for modifications. A more radical solution is to use remotely operated or autonomous vehicles, which solves the vibration problem completely by removing the operator. Considerable advances in unmanned machinery have been made, especially in the mining industry (Larsson, Broxvall and Saffiotti, 2005), and autonomous earth-moving operations in laboratory environments have been successfully demonstrated as well (Sarata, Koyachi and Sugawara, 2008). While the use of unmanned machines is likely to increase, it still seems highly probable that manned construction machines will remain in use for the foreseeable future, given the great variety in operating environments.

Given the inherent limits of current methods for vibration isolation in construction machines, it seems obvious that the logical progression is further improvement of suspension systems. With an efficient wheel suspension, surface-induced vibrations can be reduced at the source, thus improving the dynamic behaviour of the entire machine rather than merely shielding the operator. This is not only an efficient way of reducing ride vibrations, but will also reduce dynamic wheel loads, thus making higher transport speeds possible. Referring again to figure 2, this translates directly into increased productivity, since the total cycle time will be decreased. Hence, improved suspension systems will also lead to increased task performance. This is true for unmanned machines as well, as wheel load fluctuations and shaking of the carried load make higher transport velocities impractical without wheel suspension, even if no operator is

affected. Secondary effects also include reduced shock loads on the vehicle frame, which can allow lighter structural design and thereby reduced energy consumption. Decreased wheel load variation could lead to less tyre wear, as slippage is reduced. Hence, although more refined suspensions certainly mean increased procurement cost and complexity, there is much to be gained besides improved ride comfort, both economically and environmentally.

### 1.3 Research approach

As stated above, wheel suspension has the potential to improve ride comfort and productivity for a construction machine that is used to a large extent in a transporting role. However, the introduction of a more complex suspension system will also have a radical effect on the dynamic response of the machine, especially that of machines such as wheel loaders, which are traditionally built without wheel suspension. This leads to the research question considered in this thesis: *“What particular vehicle dynamic properties need to be considered in the design of a wheel suspension for a construction machine, and how is the dynamic behaviour of the machine affected by the addition of suspended wheel axles?”*

Vehicle dynamic theory provides a natural starting point for finding the answer to this question. The fundamentals of vehicle dynamic theory were first formalised in early papers on ride dynamics (Olley, 1934) and handling (Segel, 1956). These papers mark a first application of theoretical analysis in ground vehicle design. Even if the methods have evolved over time, it has been observed that many of the rules of thumb established in the early days of vehicle dynamic analysis are still adhered to by modern designers (Barak, 1991). However, the main focus of published research has been on passenger cars, to some degree extending to heavy road vehicles as well, although it has been acknowledged that the increased complexity and variety of heavy vehicles complicates the application of generic, simplified models (Gillespie and Karamihas, 2000). Another observation (Blundell and Harty, 2004) is that theoretical methods are generally applied in the early phases of a design project, while the later design stages tend to draw more from common practice and past experiences. This is a natural progression as vehicle development today takes place in increments, with each new generation differing only slightly from the previous generation. Hence, it is possible to rely on established practices and simplified design criteria.

The design of a construction machine suspension represents a different case. Rather than an incremental change, the introduction of wheel suspension systems represents a major evolutionary step in the overall design of the machine. It is therefore necessary to revisit the foundations of vehicle dynamic theory and apply these using parameter combinations relevant to construction machines. In this way, a thorough understanding of the machine dynamics can be obtained and applied to the design problem at hand. This is the philosophy behind the research presented in this thesis. Applying vehicle dynamic theory to construction machines reveals a number of areas that are critical for the dynamic behaviour of the machine, and hence illuminate certain factors that influence suspension design. This theoretical approach is complemented by simulation models and empirical testing, in order to study more complex dynamic phenomena that are not covered by elementary theoretical models.

A number of limitations have also been made. Since the main focus is suspension design, the analyses performed have been limited to ride comfort and handling stability. Longitudinal dynamics such as tractive performance have not been considered, since such properties are generally influenced more by the drive train and tyre properties than by the suspension. This also means that less attention has been paid to the particular properties of off-road terrain. While the behaviour of vehicles on deformable terrain is an important research area, it is generally more relevant to tractive performance than to ride vibrations and handling. Hence, terramechanic considerations have been deemed outside the scope of this thesis.

## 1.4 Methods used

As stated above, the objective of the research work presented here is to provide an increased insight regarding the particular vehicle dynamic behaviour of construction machines, in areas relevant to the design process for suspension systems. To this end, a number of methods on different levels of complexity have been applied.

Linearised, low-order analytical models have been utilised to study ride dynamics and lateral stability on an elementary level. This provides a fundamental understanding of dynamic behaviour and may also be used as a base for more refined analysis methods.

To study more complex dynamics, multibody dynamic simulations have been used. This allows more realistic and complex studies of the vehicle dynamic behaviour, including higher order ride dynamics and lateral dynamics such as body roll and load transfer, which are typically not covered by simplified analytical models.

Scale model testing, using a purpose-built remote-controlled vehicle, has also been used to study the lateral stability of articulated vehicles. The use of a scale model represents a compromise between cost-efficiency and accuracy, as it allows realistic experiments without the cost and complexity of full vehicle tests. Moreover, since the vehicle is unmanned, it allows the performance of hazardous tests without the safety considerations that are usually necessary in full vehicle trials.

Full vehicle testing has been utilised to a limited extent. Basic tests with an experimental suspended wheel loader, subjected to a single obstacle excitation, have been performed to gather data for comparison with multibody dynamic simulations. A rolling test rig for large tyres has also been evaluated, using a road vehicle tyre as a test object. The test results show that this test rig produces repeatable and robust tyre data and may therefore be utilised to gather data on more complex tyres as well, thus making it a useful tool for future evaluations of the dynamic behaviour of off-road tyres.

## 1.5 Outline of this thesis

The introductory part of this thesis serves as a theoretical introduction to the work presented in the appended papers, while at the same time illustrating relevant aspects of the dynamic behaviour of construction machines. The text is structured as follows.

Chapter 1 presents construction machines in general, elucidates the need for further suspension development and explains the general philosophy behind the research approach taken. Moreover, the delimitations of this work are presented here.

Ride dynamic aspects are addressed in Chapter 2. Here the particular aspects of construction machine ride dynamics are introduced from a theoretical standpoint, while at the same time introducing the analytical methods that have been utilised in **Paper A**, **B** and **C**. A number of more complex dynamic phenomena that affect ride vibrations are also discussed, with examples from the literature.

The lateral dynamics of articulated frame steer vehicles is discussed in Chapter 3. This type of steering is common on construction machines and its effects on lateral stability has therefore been analysed. The theoretical foundations are explained using a linearised model, in order to provide a fundamental view of the stability problems related to articulated vehicles. Furthermore, results from multibody dynamic simulations and scale model experiments are presented. The chapter thereby provides an introduction to the methods applied in **Paper D** and **E**.

Chapter 4 specifically discusses the dynamics of large off-road tyres. The dynamic behaviour of tyres remains an area of uncertainty in any vehicle dynamic analysis, especially in the field of off-road vehicles, since the response of large tyres is largely unknown. This chapter cites published data on various types of off-road tyres, thus presenting an empirical background for a deeper understanding of large tyre dynamics.

Chapter 5 introduces multibody dynamic simulations, a method for complex dynamic analysis that is used extensively by the vehicle industry. Multibody simulations provide a powerful way to simulate the detailed dynamics of construction machines and have been utilised in **Paper A**, **B** and **D** for analysis of both ride dynamics and lateral stability. The chapter also discusses the validation of simulation models, and describes a multibody dynamics simulation model of a wheel loader with suspended axles. This model has also been compared to measurement data that is gathered from field tests using a prototype wheel loader with similar suspension.

A summary and discussion of the research contributions made in the appended papers are presented in Chapter 6, while the main scientific contributions of the appended papers are briefly summarised in Chapter 7. Finally, Chapter 8 summarises general conclusions based on both the introductory chapters and the attached papers, and presents some recommendations for future studies.

Appendix 1 describes the evaluation of a rolling test rig for determining the characteristics of large tyres. The tyre used in the evaluation is an on-road tyre and the results are therefore not directly relevant to construction machine tyres. Hence, the main focus of the text therefore not on measurement results, but rather on how the test equipment and methods may be applied for future evaluations of off-road tyre characteristics.

## 2. Ride dynamic aspects

Ride vibrations are generally defined as tactile or visual vibrations in the frequency range of 0 to 25 Hz. Higher frequency disturbances are generally referred to as noise, and are less relevant to fundamental suspension design. Thus, the ride dynamics of a ground vehicle are mainly related to the translational and angular oscillations of the suspended mass, as caused by surface irregularities. The response of the vehicle to external excitations is directly related to the suspension properties, and can therefore be seen as the most fundamental consideration in suspension design for optimal ride characteristics.

The typical construction machine considered in this thesis is a wheeled, heavy off-road vehicle. As such, it differs in a number of respects from the road vehicles which are the focus of most published studies. Nevertheless, fundamental methods for ride analysis can provide important information on the dynamic behaviour of construction machines, if the particular differences are included in the analysis.

### 2.1 Fundamental pitch and bounce dynamics

The most elementary description of vehicle pitch and bounce dynamics is given by the two-degree-of-freedom, half-vehicle model shown in figure 3. Here the motion of the suspended mass, characterised by the mass  $m_s$  and the moment of inertia  $I_{yy}$ , is described by the vertical position  $z$  and the body pitch angle  $\theta$ . The front and rear suspension stiffness and damping are represented by  $k_1, c_1$  and  $k_2, c_2$ , respectively. The tyre stiffness and unsuspended mass oscillation are neglected. The surface excitation is introduced as the front and rear displacements  $w_1$  and  $w_2$ , respectively.

With notations from figure 3, the equations of motion for the model are in matrix form:

$$M \begin{bmatrix} \ddot{z} \\ \ddot{\theta} \end{bmatrix} + C \begin{bmatrix} \dot{z} \\ \dot{\theta} \end{bmatrix} + K \begin{bmatrix} z \\ \theta \end{bmatrix} = \begin{bmatrix} F_z \\ M_\theta \end{bmatrix} \quad (1)$$

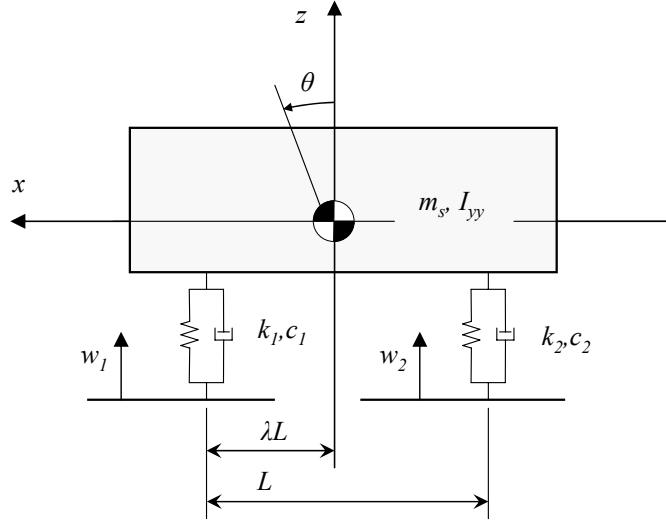


Figure 3: Two degree-of-freedom pitch and bounce model.

The matrices  $M$ ,  $K$  and  $C$  are the mass, stiffness and damping matrices of the system. Assuming linear stiffness and damping and small pitch angle displacements, these are defined as

$$M = \begin{bmatrix} m & 0 \\ 0 & I_{yy} \end{bmatrix}, \quad (2)$$

$$C = \begin{bmatrix} c_1 + c_2 & (1-\lambda)Lc_2 - \lambda Lc_1 \\ (1-\lambda)Lc_2 - \lambda Lc_1 & (\lambda L)^2 c_1 - ((1-\lambda)L)^2 c_2 \end{bmatrix}.$$

$$K = \begin{bmatrix} k_1 + k_2 & (1-\lambda)Lk_2 - \lambda Lk_1 \\ (1-\lambda)Lk_2 - \lambda Lk_1 & (\lambda L)^2 k_1 - ((1-\lambda)L)^2 k_2 \end{bmatrix}.$$

An elementary ride comfort criterion is provided by the undamped eigenfrequencies of the suspended mass. These main ride frequencies are commonly termed “pitch” and “bounce”, although the corresponding eigenmodes normally contain some degree of both pitch and bounce motions due to the off-diagonal terms in the  $K$  matrix. Nevertheless, it is common practice to name each mode after the dominating motion.

The undamped eigenfrequencies can be computed from the eigenvalues of the matrix product  $M^{-1}K$ . For favourable ride characteristics, it has been stated that the main ride

frequencies should be in the range of 1.0 to 1.3 Hz, and that the higher frequency should not be more than 20% greater than the lower. This fundamental criterion was originally stated by Maurice Olley (Olley, 1934) and has been re-iterated in later publications (Gillespie, 1992). A review of modern chassis design practices verifies that car designers still seem to adhere to this basic design principle (Barak, 1991). It could therefore be considered a simple and reasonably well-verified criterion for elementary ride design.

### 2.1.1 Dynamic index

The mass of a typical construction machine is generally in the range of 10 to 30 metric tons, higher than a passenger car or even a heavy truck. However, mass and inertia do not by themselves imply different vehicle dynamic behaviour, since the dynamic response is defined by the combination of mass and suspension stiffness, rather than the mass properties alone. A more relevant property is the relation between mass, inertia and geometry expressed as the *Dynamic Index (DI)* of the vehicle. This is defined in the pitch direction as:

$$DI = \frac{I_{yy} / m_s}{\lambda L(1 - \lambda)L} \quad (3)$$

The wheelbase  $L$  and centre of gravity position  $\lambda$  are defined as in figure 3. It can be seen that a higher  $DI$  is directly related to a large pitch inertia in combination with a short wheelbase. As seen in figure 4, this is a typical setup for wheel loaders, which feature large overhanging masses in the form of a rear-mounted engine and a front loading attachment. A similar layout can be seen in other machines that were originally based on the agricultural tractor.



Figure 4: A wheel loader with large overhanging masses at the front and rear.

The basic influence of the dynamic index on fundamental ride properties can be derived by considering the equations of motion for pitch and bounce in special case. If equal static deflections at the front and rear end are assumed, the front and rear stiffnesses are related as follows:

$$\frac{k_1}{k_2} = \frac{(1-\lambda)}{\lambda} \quad (4)$$

Scaling damping coefficients in the same manner results in the pitch and bounce motions becoming uncoupled, since the off-diagonal terms in the  $K$  and  $C$  matrices, equation (2), are zero. This means that the original equations of motion can be separated into two single-degree-of-freedom systems:

$$m_s \ddot{z} + (c_1 + c_2) \dot{z} + (k_1 + k_2)z = 0 \quad (5)$$

$$I_{yy} \ddot{\theta} + (c_1(\lambda L)^2 + c_2((1-\lambda)L)^2) \dot{\theta} + (k_1(\lambda L)^2 + k_2((1-\lambda)L)^2) \theta = 0 \quad (6)$$

From the definition of simple harmonic oscillation, the undamped eigenfrequencies  $\omega_0$  and the relative damping rates  $\zeta$  can now be identified as:

$$\omega_{0,z} = \sqrt{\frac{k_1 + k_2}{m_s}} \quad (7)$$

$$\zeta_z = \frac{c_1 + c_2}{2m\omega_{0,z}} \quad (8)$$

$$\omega_{0,\theta} = \sqrt{\frac{k_1(\lambda L)^2 + k_2((1-\lambda)L)^2}{I_{yy}}} \quad (9)$$

$$\zeta_\theta = \frac{c_1(\lambda L)^2 + c_2((1-\lambda)L)^2}{2I_{yy}\omega_{0,\theta}} \quad (10)$$

Introducing the total spring stiffness  $k_{tot} = k_1 + k_2$ , the ratio between the undamped pitch and bounce frequencies can be formulated as

$$\frac{\omega_{0,\theta}}{\omega_{0,z}} = \sqrt{\frac{(1-\lambda)k_{tot}(\lambda L)^2 + \lambda k_{tot}((1-\lambda)L)^2}{I_{yy}}} \cdot \frac{m_s}{k_{tot}} = \quad (11)$$

$$= \sqrt{\frac{m_s \lambda L(1-\lambda)L}{I_{yy}}} = \frac{1}{\sqrt{DI}}$$

The same analysis can be carried out for relative damping:

$$\frac{\zeta_\theta}{\zeta_z} = \frac{(1-\lambda)c_{tot}(\lambda L)^2 + \lambda c_{tot}((1-\lambda)L)^2}{I_{yy} \cdot 2\omega_{0,\theta}} \cdot \frac{2m_s\omega_{0,z}}{c_{tot}} = \quad (12)$$

$$= \frac{\omega_{0,z}}{\omega_{0,\theta}} \cdot \frac{\lambda L(1-\lambda)L}{I_{yy}/m_s} = \frac{\sqrt{DI}}{DI} = \frac{1}{\sqrt{DI}}$$

Hence, there is a direct relation between the dynamic index and the ratio between the eigenfrequencies and the relative damping in pitch and bounce. A higher  $DI$  leads to a pitch frequency lower than the bounce frequency and also to a lower relative pitch damping. The relationship is illustrated graphically in figure 5.

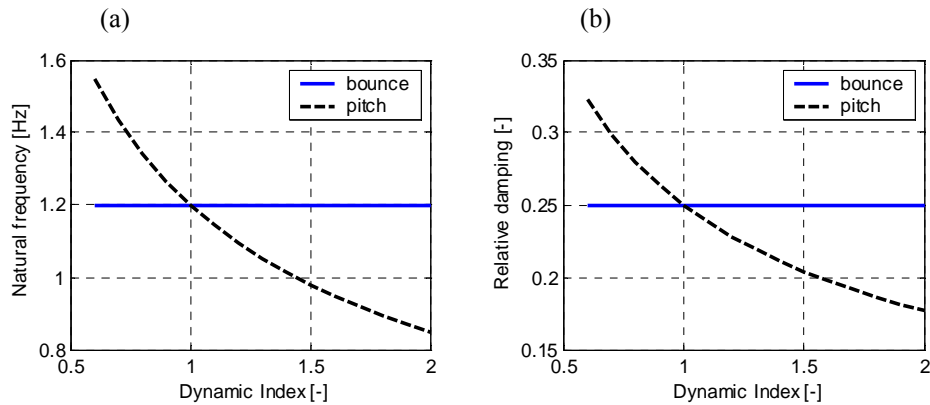


Figure 5: Relationship between the dynamic index and (a) main ride frequencies and (b) relative damping.

The relations in figure 5 offer one explanation for the typical pitch tendency seen in wheel loaders and similar vehicles that feature large pitch inertia and a short wheelbase. Since the pitch mode is generally more lightly damped, it can be expected that lightly damped pitch oscillations will dominate the free vibration of the vehicle. This is in

agreement with the observed behaviours of front loaders, especially when travelling at high speed.

Another implication of the dynamic index is the coupling between front and rear end motions. If the  $DI$  is equal to 1, the vertical motion of the front and rear end becomes completely uncoupled and the oscillation of the vehicle body can be described by two separate oscillating systems with pure vertical motion. This is a useful approximation for passenger cars, as they usually have a  $DI$  close to 1 (Heydinger et al, 1999), but it is less valid for loaders and similar vehicles with large pitch inertia and a  $DI$  typically ranging from 1.4 to 2.0. The special case of  $DI = 1$  and equal static deflections also implies that the vehicle will have a single ride frequency, as the pitch and bounce frequencies coincide. This parameter combination was at an early stage generally condemned as negative for ride comfort, since the ride becomes erratic and unpredictable (Milliken and Milliken, 2002), and is therefore mainly of theoretical interest.

### 2.1.2 Response to surface inputs

Referring back to figure 3, the surface input to the model is described by the displacements  $w_1$  and  $w_2$ , resulting in an external force and moment on the model as described by the equations

$$F_z = c_1 \dot{w}_1 + k_1 w_1 + c_2 \dot{w}_2 + k_2 w_2 \quad (13)$$

$$M_\theta = -(c_1 \dot{w}_1 + k_1 w_1) \lambda L + (c_2 \dot{w}_2 + k_2 w_2) (1 - \lambda) L \quad (14)$$

Assuming linear stiffness/damping and small angle displacements, the Laplace transform can be applied to the complete equations of motion in order to obtain the frequency-response of the model. Furthermore, it can be observed that in the general case the rear axle disturbance  $w_2$  is identical to the front input  $w_1$ , but with a time delay. In the Laplace domain, this is formulated as

$$w_2 = w_1 e^{-s\tau} \quad (15)$$

where  $\tau = L/v_x$  is the time delay between the front and rear axle excitation, when travelling at constant longitudinal velocity  $v_x$ . This makes it possible to formulate the transfer functions from a single input  $w_1$  to the bounce and pitch motions,  $H_{zw1}$  and  $H_{\theta w1}$ :

$$H_{zw1} = \frac{Z_s}{W_1} \quad (16)$$

$$H_{\theta w1} = \frac{\Theta}{W_1} \quad (17)$$

Here  $Z_s$ ,  $\Theta$  and  $W_1$  denote the frequency-domain representations of vertical motion, pitch motion and surface input, respectively.

Surface inputs are commonly described by the power spectral density (PSD) of the surface profile in the spatial frequency domain, here denoted by  $G_d$ . The standardised presentation of road roughness approximates the PSD as a function of the spatial frequency or wave number  $n$  (in the unit  $\text{m}^{-1}$ ), in the form:

$$G_d(n) = G_d(n_0) \left( \frac{n}{n_0} \right)^{-2} \quad (18)$$

This definition is specified by the ISO 8608 standard (ISO, 1995) and provides a unified input that is convenient to use in both frequency and time domain analysis. The parameter  $n_0$  is the reference frequency of  $0.1 \text{ m}^{-1}$ , while the severity of the surface roughness is determined by  $G_d(n_0)$ , which defines the PSD magnitude at  $n_0$ . Standardised parameter intervals for ISO-classified roads can be seen in figure 6.

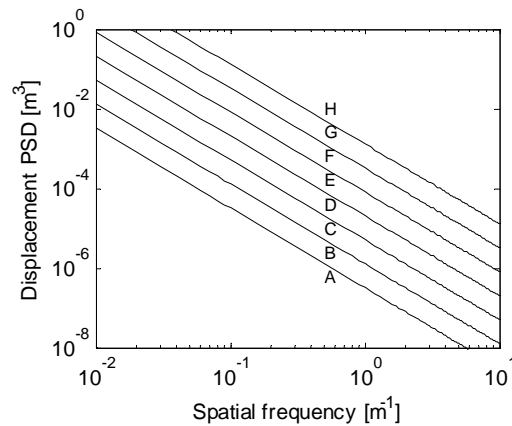


Figure 6: ISO 8608 standardised surface profiles (ISO, 1995).

Measurements show that the spectral distribution of off-road terrain may not always match the simplified description specified by ISO 8608. An example from an actual construction site (Fujimoto, 1983) is shown in figure 7 (a), together with a proposed curve fit (b). The peaks seen between  $1$  and  $10 \text{ m}^{-1}$  in the measured PSD are related to tyre tread prints. The data is presented here as an example of actual off-road terrain, but is not sufficient for general conclusions regarding off-road profiles as the detailed content of such terrain may vary considerably between measurement sites. Statistical tests have also indicated that PSD representations may not be applicable to off-road profiles, since these are not always linear, stationary and Gaussian as required by the



An example of the bounce and pitch acceleration response has been computed here for a wheel loader with parameters according to table 2, at three velocities. A full suspension is assumed, being setup for bounce and pitch frequencies at 1.2 and 1.0 Hz with equal static deflection at the front and rear end. The surface input used is an ISO 8608 C-class profile, with  $G_d(n_o) = 256 \cdot 10^{-6} \text{ m}^3$ . The results are displayed in figure 8.

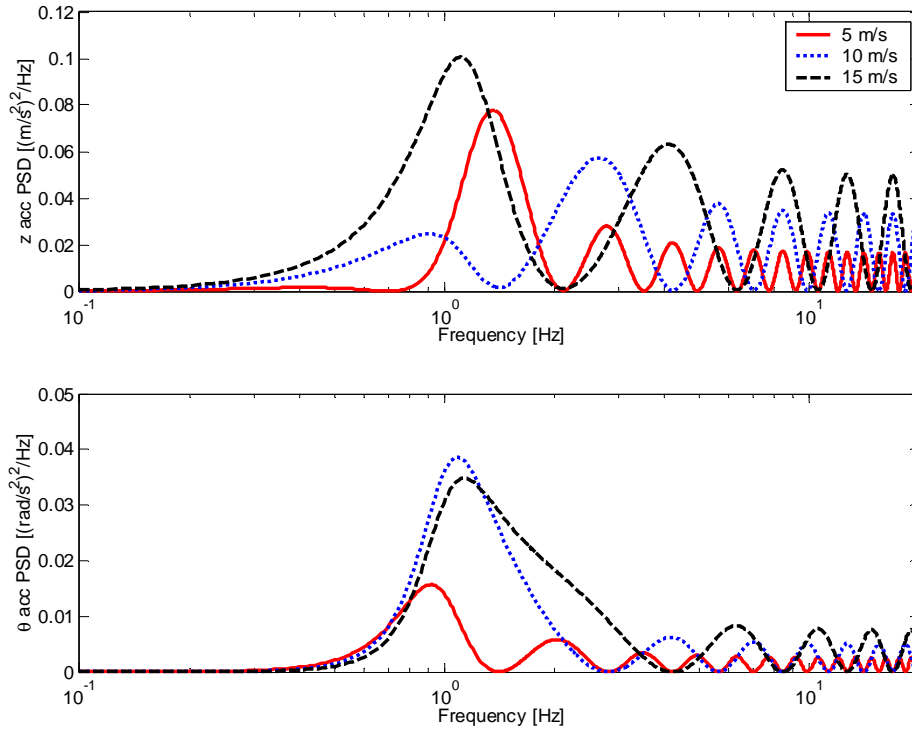


Figure 8: Acceleration PSD in bounce and pitch for a medium-sized wheel loader with suspended axles.

Table 2: Vehicle parameters for a wheel loader with suspended axles.

Parameter	Value
Suspended mass $m_s$	22,000 kg
Wheelbase $L$	3.55 m
Centre of gravity position $\lambda$	0.45
Dynamic index $DI$	1.44
Undamped bounce frequency $f_{0,z}$	1.20 Hz
Undamped pitch frequency $f_{0,\theta}$	1.00 Hz
Relative bounce damping $\zeta_z$	0.38
Relative pitch damping $\zeta_\theta$	0.31

It can be seen in figure 8 that the spectral distributions are highly dependent on the velocity, due to the wheelbase filtering effect. The combination of low velocity and a long wheelbase makes wheelbase filtering prominent at frequencies close to the resonance peaks, thereby shaping the response at low frequencies. For example, the largest peak in the vertical acceleration PSD at 10 m/s occurs around 2.6 Hz because of wheelbase filtering at 1.4 Hz, near the resonance frequency. To some degree, this complicates ride comfort optimisation for a construction machine, since the frequency response can be expected to be influenced by the vehicle velocity as well as by the suspension setup. It can also be noted that the peak acceleration response does not always occur near the main ride frequencies.

### 2.1.3 Suspension setup for minimised pitch response

As explained above, many construction machines can be expected to exhibit prominent pitching oscillation because of a high dynamic pitch index. It is therefore of interest to examine how a wheel suspension can alleviate the pitching tendency of the machine. Suspension design for “flat ride”, or minimised pitch response, was first introduced in an early paper by Olley (1934). The design concept is based on the observation that the road excitation of the rear axle is the same as that of the front axle, but with a given time delay. This leads to a phase shift between the front and rear end oscillations. If the frequency of oscillations is higher at the rear end, the motions of the front and rear end will combine into a bounce-dominated motion of the suspended mass. Hence, a decrease in pitch oscillation will occur while the vertical acceleration increases. This is obtained in practice by selecting a stiffer rear suspension, sometimes referred to as an “Olleyed” setup, whereas the opposite is termed a “reverse Olley” setup. While the original guideline was mainly based on experimentation and intuitive reasoning, it has later been thoroughly validated by frequency response analysis (Best, 1984; Sharp and Pilbeam, 1993); and it has also been analytically proved that minimum pitch and vertical response are contradicting design objectives (Sharp, 2002). A general observation is also that a flat ride setup is more easily attainable at higher velocities.

It should be noted that the reasoning behind the flat ride setup assumes isolated vertical displacements of the front and rear end of the vehicle. This implies a vehicle with  $DI = 1$ , which was also used in the theoretical studies cited above. For such a vehicle, the front and rear stiffness can be converted directly into natural frequencies of the front and rear ends. As already stated, this is normally not the case for a construction machine, although it has been stated that an Olleyed setup reduces the pitching motion for a vehicle with  $DI > 1$  as well, as long as the rear suspension stiffness is sufficiently greater than the front suspension stiffness (Gillespie, 1992).

The potential for the flat ride setup has been investigated here for a fully suspended wheel loader with the parameters from table 2 and a velocity of 15 m/s. The total stiffness  $k_1 + k_2$  has been kept constant, while the ratio  $k_2/k_1$  has been varied from the original setting of 0.818, corresponding to decoupled pitch and bounce motions, to a higher rear stiffness. The damping coefficients have been scaled accordingly. The resulting PSD of the vertical and pitch accelerations are seen in figure 9.

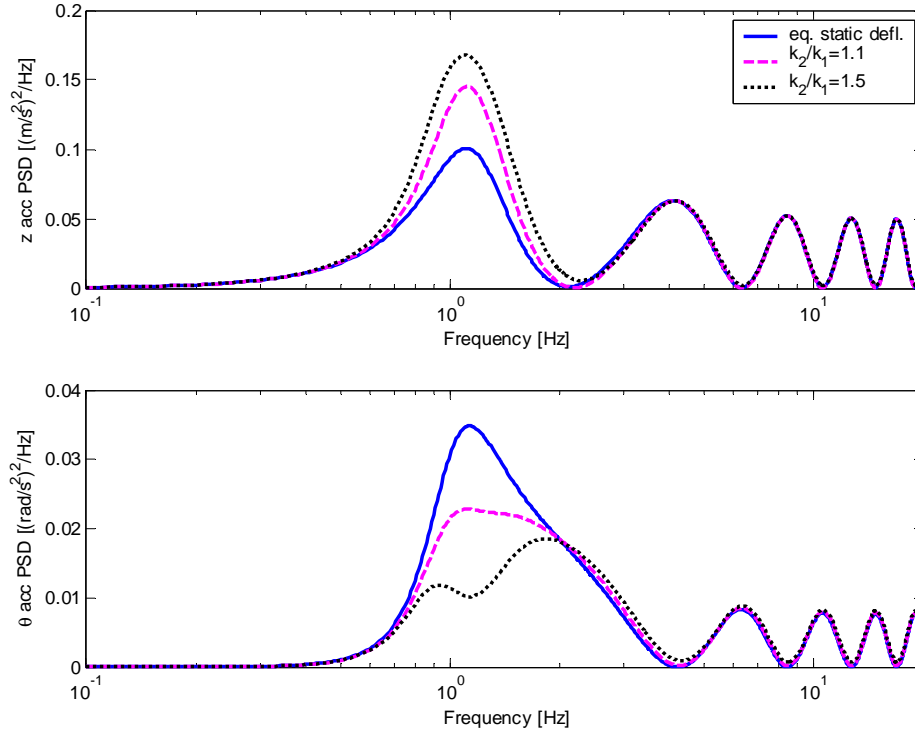


Figure 9: Acceleration PSD for different suspension setups, showing “flat ride” effect.

It can be seen in figure 9 that the peak in the pitch acceleration PSD is reduced with stiffer rear suspension, although the response at higher frequencies is largely unaffected. Conversely, the peak vertical acceleration response becomes larger, as expected. An altered spring setup will also affect the natural frequencies. The undamped pitch and bounce frequencies for the setups analysed are summarised in table 3. It is seen that  $k_2/k_1 = 1.5$  leads to undesirable separation between natural frequencies, thus impairing the possibility for pitch response reduction. Static deflections may also be impractically large using this setup.

The RMS accelerations, as presented in table 3, have been computed by integrating the PSD distributions over the frequency range from 0 to 20 Hz. It is seen that the RMS values are almost unaffected by the suspension setup, which is reasonable since the PSD distribution is mainly affected near the peak response, as seen in figure 9.

Table 3: Natural frequencies for different suspension setups.

Setup	Bounce frequency	Pitch frequency	RMS $z$ acceleration	RMS $\theta$ acceleration
Decoupled	1.20 Hz	1.00 Hz	0.74 m/s <sup>2</sup>	0.34 rad/s <sup>2</sup>
$k_2/k_1 = 1.1$	1.23 Hz	0.98 Hz	0.76 m/s <sup>2</sup>	0.33 rad/s <sup>2</sup>
$k_2/k_1 = 1.5$	1.29 Hz	0.92 Hz	0.79 m/s <sup>2</sup>	0.33 rad/s <sup>2</sup>

#### 2.1.4 Effects of load change and ride height control

Construction machines are designed for high amounts of mass compared to the vehicle weight. Dedicated transport vehicles such as dump trucks are often intended to carry loads exceeding the empty weight of the machine, thus leading to axle loads increasing by 100% or more when loaded. For a front loader, increased loading also means a large displacement of the centre of gravity, since the load is carried ahead of the front axle. This means that the axle loads of the machine can be expected to differ considerably between the loaded and the unloaded configuration.

To analyse this effect, the changes in axle loads have been calculated for a wheel loader with the parameters from table 2 and an added mass of 6,900 kg, carried in the loader bucket 1.0 m ahead of the front axle. The pitch inertia for the loaded machine has been computed using the parallel axis theorem, simplifying the bucket load to a point mass. The resulting changes in the loads and mass properties are shown in table 4.

Table 4: Changes in parameters used for the loaded wheel loader.

Parameter	Unloaded value	Loaded value
Suspended mass $m_s$	22,000 kg	28,900 kg
Centre of gravity position $\lambda$	0.45	0.28
Dynamic index $DI$	1.44	1.85
Front axle load	119 kN	204 kN
Rear axle load	97 kN	79 kN

It can be seen that the rear axle load decreases by about 20%, while the front axle load is increased by about 70%. Unless the springs are selected with a very high stiffness, some form of ride height adjustment is necessary to handle the loaded condition. Analysed here are two basic applications of gas springs, which are capable of accommodating load changes by adjusting the equilibrium position of the suspension. The two configurations are shown schematically in figure 10 (Harrison, 1983).

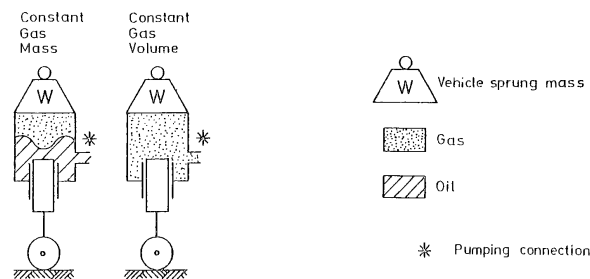


Figure 10: Principles for gas springs of different design (Harrison, 1983).

The basic idea of ride height control is to adjust the equilibrium position of the suspension so that the deflection is constant regardless of the applied load. Depending on the application, this will affect the spring stiffness in different ways.

#### *Constant mass gas spring*

In this type of suspension, the suspension displacement acts on the gas spring through a volume of oil. The spring element itself consists of a sealed gas accumulator that is separated from the oil volume by a rubber membrane. The ride height adjustment is achieved by altering the amount of oil in the system, thereby compensating for the change in gas volume at equilibrium. Since the force-deflection relationship of the gas spring is nonlinear and progressive, the stiffness of the spring will increase with the load. The linearised stiffness  $k_{cm}$  of an ideal constant mass gas spring is given by (Harrison, 1983):

$$k_{cm} = \frac{\kappa(N + p_A A_p)^2}{n_{gas} RT} \quad (22)$$

where  $N$  is the force acting on the spring,  $p_A$  is the atmospheric pressure and  $A_p$  is the effective area of the spring piston. The polytropic index  $\kappa$ , the molar gas quantity  $n_{gas}$ , the universal gas constant  $R$  and the gas temperature  $T$  are assumed to be constant. Hence, if the term  $p_A A_p$  is small compared to  $N$ , the spring stiffness is proportional to the square of the axle load  $N$  when linearised around an equilibrium position.

#### *Constant volume gas spring*

A constant volume gas suspension compensates for changes in the static load by altering the amount of gas in the system. Thus, the static deflection is maintained by keeping the gas volume unchanged. The linearised stiffness  $k_{cv}$  of a constant volume gas spring follows the relation (Harrison, 1983):

$$k_{cv} = \frac{\kappa A(N + p_A A_p)}{V_E} \quad (23)$$

Here  $V_E$  is the equilibrium gas volume, which is kept constant by the system. As in the case of the constant mass gas spring,  $p_A A_p$  can usually be neglected and the spring stiffness is therefore in this case linearly dependent on the axle load  $N$ .

For both systems described above, the spring stiffness is altered with the load. Hence, the response of the vehicle will change when in a loaded condition. The exact nature of the change will depend on the type of suspension selected. The suspension properties for the loaded machine have been computed for a wheel loader with the parameters from table 2, equipped either with constant mass or constant volume gas springs. The suspension is set up so that, in unloaded condition, the rear suspension is 1.1 times

stiffer than the front suspension. This is in accordance with the flat ride design principle described above. Table 5 also shows the resulting suspension properties when loaded, together with the undamped pitch and bounce frequencies.

Table 5: Changes in suspension properties with load.

Parameter	Unloaded	Loaded, constant mass springs	Loaded, constant volume springs
Front stiffness $k_1$	596 kN/m	1,911 kN/m	1,031 kN/m
Rear stiffness $k_2$	655 kN/m	349 kN/m	527 kN/m
Stiffness ratio $k_2/k_1$	1.1	0.18	0.51
Bounce frequency $f_{0,z}$	1.23 Hz	1.45 Hz	1.18 Hz
Pitch frequency $f_{0,\theta}$	0.98 Hz	0.81 Hz	0.90 Hz

It can be seen in table 5 that in both cases, the front suspension stiffness has increased, while the rear suspension stiffness has decreased. This is caused by the changes in the axle loads, as seen in table 4. Moreover, this alters the relative stiffness between the front and rear suspension, in both cases resulting in a “reverse Olley” setup by means of stiffness ratio, since the front suspension stiffness is now higher than the rear stiffness. The natural frequencies are also affected, offsetting the original setup. This is more noticeable in the case of constant mass springs.

Figure 11 shows the PSD of bounce and pitch acceleration for the wheel loader, unloaded and loaded, with the two different suspension systems. The damping coefficients ( $c_1$ ,  $c_2$ ) are kept constant. For the constant mass system, it is seen that both responses are amplified considerably in the loaded condition due to increased spring stiffness. The constant volume system also gives increased resonance in vertical acceleration, although the effect is less dramatic. The pitch response of the constant volume suspension is higher at the resonance peak, but is actually lower than for the unloaded machine at 1 Hz and higher frequencies.

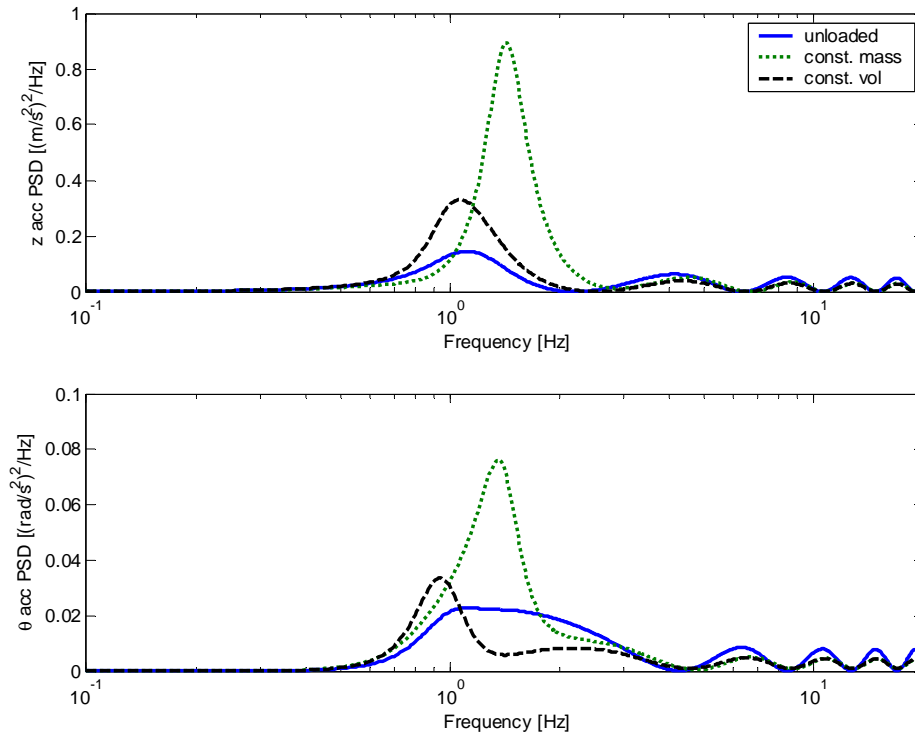


Figure 11: Acceleration response of wheel loader for unloaded vehicle, for loaded vehicle with constant mass suspension and for loaded vehicle with constant volume suspension.

The increased response of the loaded vehicle is caused by a generally higher spring stiffness and an unbalanced (reverse Olley) suspension setup, but is also influenced by the decrease in relative damping. Since relative damping is inversely proportional to mass and inertia, as seen in equations (8) and (10), increasing these will lead to a lower relative damping if the damping coefficients are kept constant. Hence, adjusting the damping with the load could reduce the acceleration response in the loaded condition.

While the results above indicate that the constant volume system is more desirable from a vehicle dynamic standpoint, such an installation may also lead to increased costs and complexity, since auxiliary systems are required for gas flow control and pressure regulation. A constant mass system can more easily be integrated with the hydraulic system of the machine, thus requiring fewer modifications. Load-sensitive damping could also be a possible way to achieve acceptable ride quality despite the limitations of the constant mass springs, thus obtaining adequate dynamic response with a less complex system.

### 2.1.5 The influence of the tyres on pitch and bounce dynamics

The pitch and bounce model used in the analysis presented in Sections 2.1.1 - 2.1.4 neglects tyre flexibility, assuming that suspension springs are the main flexible elements of the model. In practice, construction machine tyres are large and soft compared to road vehicle tyres, meaning that large deflections may occur in the tyres as well as in the main suspension. There is also a considerable span in tyre parameters, as specialised applications demand different tyre types. Furthermore, the unsuspended mass of a construction machine is relatively high, since the components need to be designed to withstand large loads. This makes it relevant to investigate the effect of tyre compliance and unsuspended mass dynamics on fundamental vehicle response.

To include the tyres and unsuspended mass in the ride analysis, the 2-DOF model in figure 3 is expanded to create the 4-DOF model seen in figure 12. Here the vertical motions of the unsuspended masses  $m_{u1}$  and  $m_{u2}$  have been included. Tyre stiffness and damping are represented by the linear stiffness and damping coefficients  $k_t$  and  $c_t$ , respectively. Note that these values represent the total stiffness per axle, i.e. for two tyres.

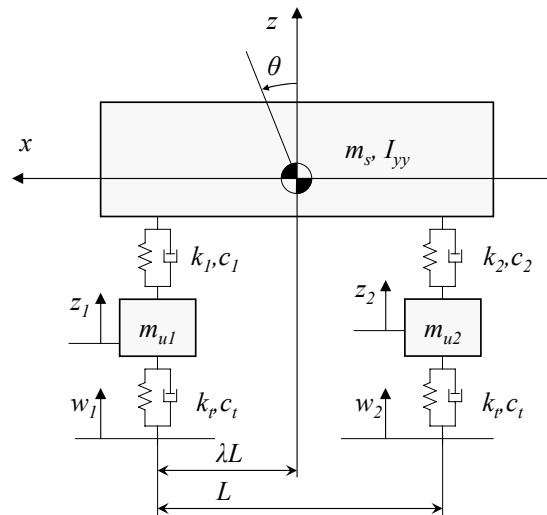


Figure 12: Pitch and bounce model including tyre stiffness/damping and unsuspended masses.

The suspension stiffness and damping are the same that are used for the 2-DOF model with uncoupled pitch and bounce motions. The tyre stiffness  $k_t$  and damping  $c_t$  per axle are assumed to be 3100 kN/m and 31 kNs/m respectively, while the unsuspended masses  $m_{u1}$  and  $m_{u2}$  are assumed to be 2,700 kg each. The vertical and pitch accelerations for the 4-DOF model have been computed in the same way as those of the 2-DOF model, using the ISO C-class road as the excitation source and 15 m/s as the velocity. The resulting responses are shown in figure 13.

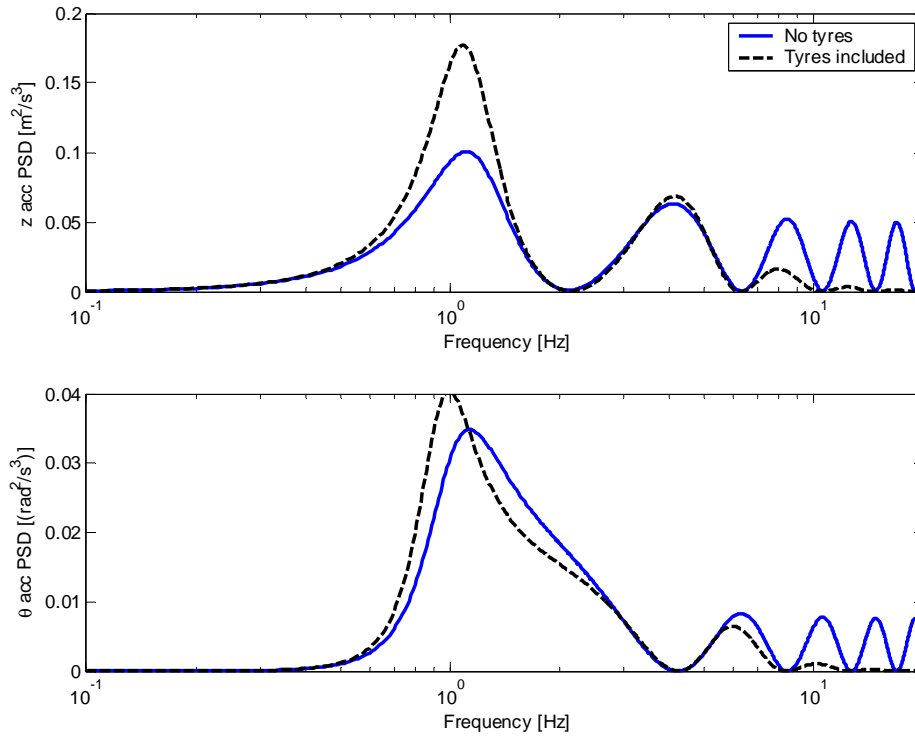


Figure 13: Acceleration PSD in bounce and pitch for 4-DOF model, including tyre characteristics.

In general, the acceleration is higher near the resonance peaks, but lower throughout the higher end of the frequency range. The shape of the curves in figure 13 therefore indicates that the overall damping is lowered, since increased damping generally has the effect of decreasing the response near the resonance frequency while increasing the response for higher frequencies. Apparently, the low tyre damping reduces the damping of the suspended mass oscillations as well. Apart from the peaks near the resonance frequencies, no obvious peaks related to unsuspended mass oscillations can be seen. Hence, the unsuspended mass bounce modes seem to be well attenuated despite the low tyre damping. The undamped natural frequencies of the 4-DOF model can be calculated in the same way as those of the 2-DOF model, and are shown in table 6.

Table 6: Comparison of undamped natural frequencies.

Mode	4-DOF model	2-DOF model
Suspended mass bounce	1.09 Hz	1.20 Hz
Suspended mass pitch	0.91 Hz	1.00 Hz
Front axle bounce	5.98 Hz	-
Rear axle bounce	5.87 Hz	-

It is seen that the inclusion of the tyre stiffness in the model results in lower main ride frequencies, which is to be expected since the tyre stiffness lowers the combined stiffness, or ride rate, of each axle. Figure 14 shows how varying tyre stiffness affects the undamped natural frequencies for the model in figure 12, computed for a combined tyre stiffness  $k_t$  ranging from 1,550 kN/m to 6,200 kN/m per axle. This can be considered a reasonable range, given the large variety of construction machine tyres. It can be seen that an increase of 50% from the baseline tyre stiffness of 3,200 kN/m results in an increase of about 3% in the pitch and bounce frequencies. The influence is larger with very low tyre stiffness.

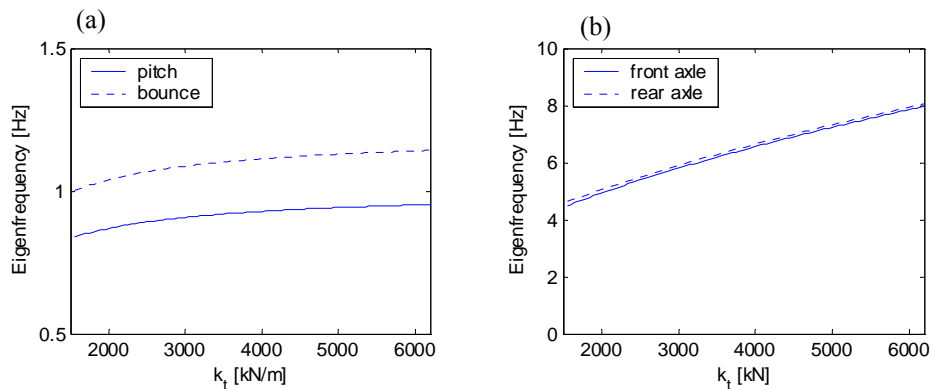


Figure 14: Influence of tyre stiffness on (a) main ride frequencies and (b) wheel hop frequencies for the front and rear axles.

Further effects of the tyre properties on the ride dynamics are analysed in greater detail in **Paper C**. A more detailed review of empirically determined tyre characteristics, including frequency- and velocity-dependent characteristics, is presented in Chapter 4.

## 2.2 Roll dynamics

The fundamental roll dynamics can be analysed with a methodology similar to the pitch and bounce analysis presented in Section 2.1. As in the case of the pitch and bounce frequencies, it is desirable to maintain a roll frequency in the range of 1.0 to 1.3 Hz for optimal ride comfort (Gillespie, 1992). However, roll comfort generally represents a more difficult case than pitch and bounce comfort, since the effective roll stiffness is also governed by the handling stability. It can be shown that the rollover stability margin decreases with the roll angle (Dukkipati et al, 2008), and it has also been observed that the roll angle displacement may be used as a measure of the handling stability (Uys, Els and Thoresson, 2004). This means that high roll stiffness is desirable from a stability standpoint. Furthermore, the design of construction machines often places the centre of gravity in a high position, especially when loaded (as seen in figure 15). The inertial forces therefore create an overturning moment which needs to be compensated for by sufficient roll stiffness. This is often detrimental to ride comfort, as

it leads to high lateral accelerations when the vehicle is subjected to large asymmetric surface disturbances.



Figure 15: Wheel loader and articulated dump trucks with high positioned loads.

Given the conflicting demands for ride comfort and rollover stability, especially on uneven surfaces, it seems unlikely that a passive system can fulfil both requirements. Thus, a semi-active or active system may be necessary. Such systems have the capability to reduce large roll displacements when there are transient loads, while maintaining low accelerations in normal driving. Although the majority of research work on active systems has been carried out for road vehicles, some examples exist where the technology has been applied to off-road vehicles. Semi-active systems have been demonstrated for agricultural tractors (Sarami, Meyer and Hammes, 2008), as well as for military off-road vehicles (Els et al, 2007), and have been seen to reduce transient roll motion while at the same time minimising lateral accelerations. Fully active roll control in the form of an active anti-roll bar has also been implemented on an off-road passenger vehicle (Cronjé and Els, 2010), and was seen to improve the handling stability with preserved ride comfort. One particular concern for construction machines is the large loads involved in active ride control. This may restrict the possibility for active control, possibly limiting the potential for control to semi-active damping.

### 2.3 Higher order dynamics

Besides the elementary oscillations of the suspended and unsuspended mass, other resonances may exist in the frequency range relevant to ride comfort. One cause of such vibrations is individual components attached to the vehicle frame, as the large masses of these components lead to relatively low natural frequencies. An overview of resonance modes in heavy trucks has been presented by Gillespie (1985), who has listed a number of component resonance modes in the 1 to 20 Hz range, for example exhaust stack longitudinal oscillation (6.9 Hz), radiator pitching (10.1 Hz) and cab bouncing (15.2 Hz). This condition is similar to that for construction machines, which feature a number of components of high mass such as the cab, lifting attachment and driveline assembly. As construction machines may vary considerably in layout and size, the exact spectrum of vibrations is highly individual for each machine type and needs to be determined using modal analysis methods.

Elastic deformation of the vehicle frame is also a source of low frequency vibration in heavy vehicles, the most typical example being the bending and torsion of the longitudinal frame members in heavy trucks. Such flexible modes are said to occur at 6-10 Hz (Gillespie, 1985). Similar conditions exist in buses, where structural optimisation of the upper body has been shown to improve ride comfort (Eriksson, 2001). Finite element studies of an articulated dump truck frame (Guo et al, 2008) have shown a first bending mode at 10.2 Hz and a first torsion mode at 17.4 Hz. As these modes are computed on the bare frame, it seems likely that the resulting frequencies are lower on the full vehicle, as attached masses lower the resonance frequency.

From the simulations and studies cited above, it can be concluded that higher order modes exist and most likely influence the ride dynamics, but that such modes generally occur at frequencies above the main ride frequencies which are important in suspension design. Furthermore, many of the higher order modes are consequences of fundamental layout decisions and are therefore difficult to change, unless a major vehicle redesign is undertaken. Thus, the higher order modes are best considered as boundary conditions for suspension design, rather than a part of the design space.

### 3. Lateral dynamics of articulated frame steer vehicles

Articulated frame steering, the principle of which is illustrated in figure 16, is commonly used on wheeled construction machines. Instead of applying the steering angle to the wheels, the steering of an articulated frame vehicle is achieved by changing the relative yaw angles of the front and rear vehicle parts, which are connected by a centre joint. Normally hydraulic cylinders are used to accomplish this, although mechanical solutions exist for smaller vehicles. Articulated steering is said to have been first patented in the early twentieth century (Holm, 1970).

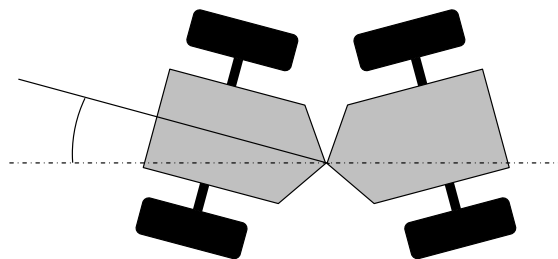


Figure 16: Principle of articulated frame steering.

Articulated steering allows a smaller turning radius than traditional, Ackermann-type steering and is also a robust installation as no steering rods or similar components need to be integrated in the wheel-axle assembly. A known drawback is the reduced rollover stability at standstill, caused by lateral shifting of the centre of gravity. Besides its installation in construction machines, the steering type can be found on various agricultural and forestry machines, as well as specialised off-road transport vehicles.

### 3.1 Planar analysis

The in-plane dynamics of an articulated vehicle can be described by the model seen in figure 17. The vehicle frames are represented by the two rigid bodies with masses and moments of inertia denoted by  $m_1, I_1$  and  $m_2, I_2$ . The position vector  $(x_1, y_1)$  describes the motion of the front frame in an earth-fixed system, while the longitudinal and lateral velocities  $u$  and  $v$  quantify the front frame velocities in body-fixed coordinates.

The torsional stiffness and damping  $K_R$  and  $C_R$  represent the equivalent stiffness of the hydraulic steering system, which is assumed to have some degree of flexibility due to oil compressibility and component elasticity. This torsional spring and damper element acts around an equilibrium position corresponding to the set steer angle. In straight line driving, this angle is zero.

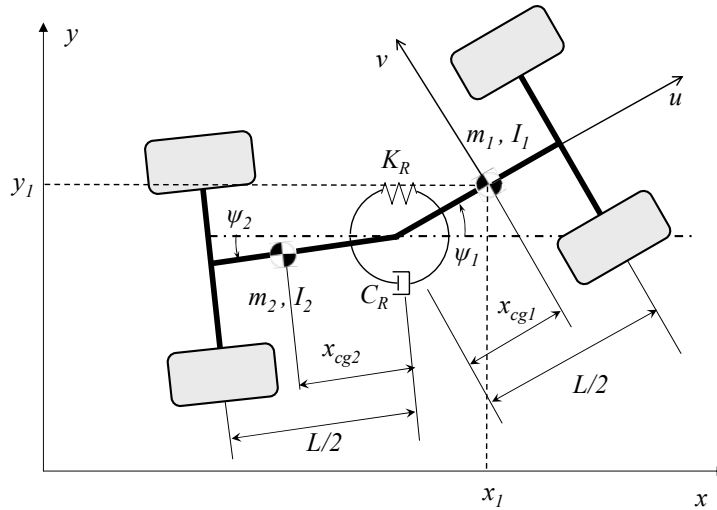


Figure 17: Planar model for lateral analysis of an articulated frame steer vehicle.

The articulation angle  $\varphi$  is defined as the difference in yaw angle between the front and rear frames, i.e.:

$$\varphi = \psi_1 - \psi_2 \quad (24)$$

The front and rear tyre forces  $F_{y,1}$  and  $F_{y,2}$  are assumed to be linear functions of the slip angle  $\alpha_i$ , so that:

$$F_{y,i} = C_i \alpha_i \quad (25)$$

A similar relation defines the front and rear aligning moments  $M_{z,1}$  and  $M_{z,2}$ :

$$M_{z,i} = C_{Mi} \alpha_i \quad (26)$$

The parameters  $C_1$ ,  $C_2$  and  $C_{M1}$ ,  $C_{M2}$  define the cornering stiffness and aligning moment coefficients of the front and rear tyres, respectively.

Assuming small articulation angle and a constant longitudinal velocity,  $u$ , the equations of motion of the vehicle model in figure 17 can be expressed as a linear system of first order equations, in the form

$$\dot{x} = Ax \quad (27)$$

where the state vector  $\dot{x}$  is given by

$$x = \begin{bmatrix} v \\ \dot{\psi} \\ \dot{\phi} \\ \phi \end{bmatrix} \quad (28)$$

The matrix  $A$  is dependent on the vehicle parameters, as well as the longitudinal velocity  $u$ , since this velocity implicitly defines the tyre forces. A full derivation has been presented by Azad, McPhee and Khajepour (2005a). The entries of the  $A$  matrix are also found in **Paper E**.

The in-plane stability properties of the vehicle can be analysed on a fundamental level by studying the eigenvalues of the system matrix  $A$ . Any eigenvalue with a positive real part will indicate a divergent or unstable mode. Furthermore, a purely real eigenvalue will correspond to an exponentially divergent or decaying mode, whereas eigenvalues with nonzero imaginary parts signify an oscillatory motion (Azad, McPhee and Khajepour, 2005a). These two modes have been termed “folding” and “snaking” (Crolla and Horton, 1983), in accordance with their physical interpretation. Examples of eigenvalue analysis can be seen in figure 18. Here the method described above has been applied to the model in figure 17, with parameters corresponding to those of an articulated tractor (Crolla and Horton, 1983), and with a total mass of 3,000 kg and identical front and rear frames. The real part of each eigenvalue has been plotted against the vehicle velocity. In the graph, crosses symbolise purely real eigenvalues while dots indicate eigenvalues with an imaginary component. A total of four eigenvalues exist. As complex eigenvalues appear as conjugates, only one point appears in the graph for each pair of eigenvalues.

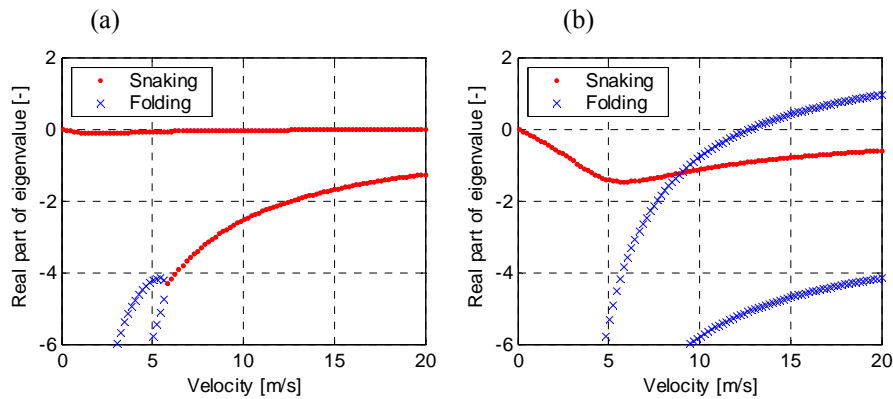


Figure 18: Eigenvalue analysis for an articulated tractor, showing folding (blue, crosses) and snaking (red, dots) eigenvalues in (a) baseline setup and (b) setup with centres of gravity closer to the centre joint.

In figure 18 (a), two real eigenvalues can be seen at velocities below 6.0 m/s. These correspond to strongly damped modes dominated by the lateral velocity  $v$ , thus indicating a divergent lateral motion. The two complex eigenvalues seen at low velocities have small negative real parts, and therefore indicate a lightly damped oscillatory mode dominated by oscillations in the articulating angle  $\varphi$ . At higher velocities, only complex eigenvalues exist, appearing as two conjugated pairs. These two eigenvalues indicate that one lightly damped or slightly divergent oscillatory mode exists, as well as a similar, more strongly damped mode. Figure 18 (b) shows an analysis with similar parameters, but with the centre of gravity positions moved closer to the centre, so that the centres of gravity are located between the respective axles and the central joint. It can be seen that two divergent modes exist, one of which becomes unstable at 12.5 m/s, as the eigenvalues become positive at this point. The oscillatory mode is stable throughout the velocity range for this configuration.

Using the method outlined above, Crolla and Horton (1983) investigated the influence of vehicle parameters on snaking and folding behaviour. Generally the most important parametric influences can be summed up as follows:

- *Mass and inertia*: Eigenvalue analysis showed that increased inertia of the rear frame decreases the stability. Increased rear frame mass has a similar but less pronounced effect.
- *Centre of gravity positions*: Moving the rear frame's centre of gravity further aft deteriorates the snaking stability in the same manner as increasing the rear frame inertia. Moreover, moving the centres of gravity closer to the centre joint seemed to reduce the margin for folding instability.
- *Steering system properties*: It was found that a lower equivalent stiffness ( $K_R$ ) resulted in highly deteriorated stability. In practice, decreased stiffness may occur because of air inclusion in the hydraulic system. Hence, this is highly undesirable with regard to snaking stability. It was also found that increased equivalent damping ( $C_R$ ) results in a more stable vehicle.

The effect of mass distribution is particularly important for a construction machine, since there may be a considerable difference between the loaded and unloaded condition. For a loader, it can be expected that the vehicle will be rear heavy when travelling unloaded, and hence it is most prone to snaking instability in this configuration. An articulated dump truck is loaded closer to the vehicle centre, and hence could be expected to display increased tendency towards folding when loaded.

## 3.2 Expanded linear analysis

A more refined study using the planar model was later published by Horton and Crolla (1986). Here a full model of the hydraulic steering system was included, replacing the simple equivalent torsion and damping seen in figure 17. Using this model, it was shown that, besides the snaking and folding modes, a third, “oversteering” mode also exists. This mode takes the form of a slow divergence in the articulation angle. It was hypothesised that this “oversteering” divergence may be the true cause of snaking oscillations, as an effect of the driver overcorrecting in order to maintain a straight path. Later full vehicle tests conducted with a wheel loader on a paved road (Lopatka and Muszynski, 2003) supports this to some extent, since the main frequency of snaking oscillation seemed there to occur at 0.1 Hz, which matches the primary frequency of driver inputs. Hence, the low frequency snaking behaviour seen in the tests could well be the effect of driver corrections, as suggested by the results from the expanded planar analysis.

## 3.3 Multibody dynamic simulations

### 3.3.1 Related work

More recently, studies of snaking and folding have been presented based on multibody dynamic simulations. Azad, McPhee and Khajepour (2005a) investigated the dynamics of an articulated forest machine, using both multibody simulations and linear predictions. The simulation results generally confirm the linear predictions, although some discrepancies were noted due to tyre nonlinearities not present in the planar model. A similar study showed that the longitudinal forces during snaking oscillations are small compared to the lateral forces (Azad, Khajepour and McPhee, 2005b), indicating that drive configuration is less relevant to snaking stability. Furthermore, both linearised theory and multibody simulations indicated that locked differentials stabilise snaking oscillation (Azad, Khajepour and McPhee, 2007). Dudzinski and Skurjat (2010) used a multibody dynamic model of a wheel loader for stability analysis focusing particularly on the steering system stiffness and also on the drive configuration. It was seen that decreased steering stiffness has a negative impact on stability, as found in previous studies, but also that front-wheel drive results in a more stable vehicle than rear- or all-wheel drive, contrary to previously published simulation results.

### 3.3.2 Investigation of the suspension's influence

Multibody dynamic simulations have been used in **Paper D** to investigate the effect of suspended axles on the lateral stability of an articulated vehicle. With suspended axles, it can be expected that the suspended mass roll will interact with snaking oscillations, possibly influencing the snaking stability. This effect is not covered by the planar model in figure 17 and therefore requires a model with more degrees of freedom.

The model used in **Paper D** is a simplified model of a wheel loader, seen in figure 19. To simulate suspended mass roll, the model uses an equivalent roll stiffness approximation of the wheel suspension, modelled using rigid axles pivoting around the centre of each axle. Thus, the suspended mass has the freedom to roll, but not to pitch or bounce except on the tyres. The suspension roll stiffness is represented by an equivalent torsion stiffness acting around the roll centres, located in the middle of each axle, while the steering system flexibility is simulated by a centre torsion stiffness in the same way as in the planar model (figure 17). The masses of the front and rear parts are assumed to be 7,200 kg and 12,000 kg, respectively. The wheelbase is 3.6 m and the track width is 2.4 m.

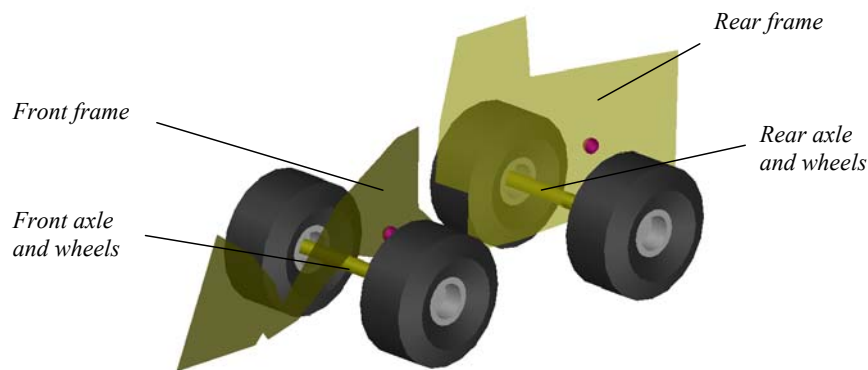


Figure 19: Multibody simulation model used in Paper D.

Analysis of the snaking stability is performed by simulating the vehicle going straight forward on a level surface at a constant velocity, and initiating a snaking oscillation by a steering torque applied at the centre joint. The baseline suspension is set up so that the undamped suspended mass roll frequency is 1.00 Hz, while the relative roll damping is approximately 0.10. An unsuspended configuration is also analysed for comparison. In this configuration, the front axle is locked to the front frame while the rear axle is allowed to pivot freely about the roll centre.

Figure 20 shows a comparison between the responses of the suspended and unsuspended models after an initial steering disturbance at 6 s, when evaluated at a velocity of 10 m/s. It is seen that the articulation angle slowly diverges for the suspended vehicle, as compared to the near-neutral stable unsuspended configuration. In addition, the frequency of the snaking oscillations is slightly decreased. This seems

to indicate that the snaking and rolling motions of the suspended vehicle behave in a coupled manner, so that the combined yaw and roll inertias lead to a lower frequency compared to the pure yaw oscillations of the unsuspended vehicle.

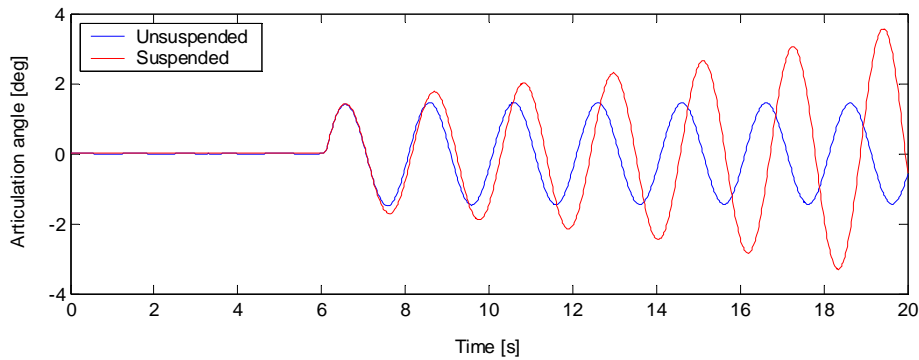


Figure 20: Articulation angle time history from multibody simulations.

Further investigation of the snaking and rolling motions shows that body roll and snaking motion are closely connected, as seen in figure 21. Both angles exhibit a harmonic oscillation at almost the same frequency, with the roll angle showing some time delay. Changing the roll stiffness does not affect the roll frequency during snaking to any greater extent. Hence, the snaking motion of the suspended vehicle can be characterised as a combination of yawing and rolling motions with closely matched frequencies.

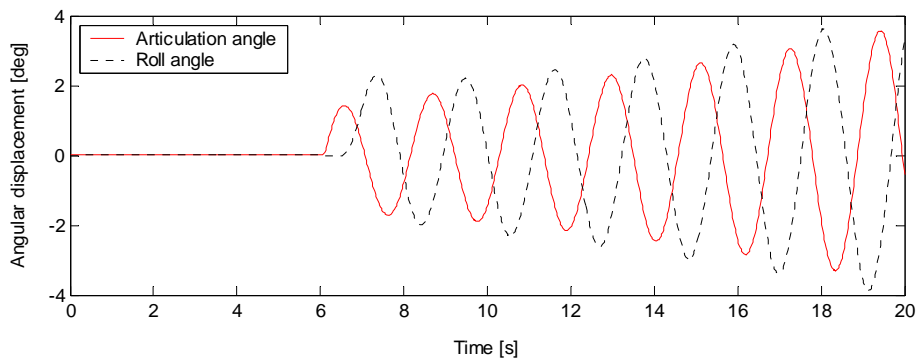


Figure 21: Articulation and roll angle time history.

As the rolling and snaking motions are closely coupled, it can be expected that the stability will be most affected when the eigenfrequency in roll coincides with the snaking frequency. This is investigated in further detail in **Paper D**. It is found that minimum stability occurs when the suspended mass roll resonance is set to a value similar to the snaking frequency, but that the effect is generally small and can be offset by small changes in other parameters, such as mass and inertia or steering system stiffness.

### 3.4 Scale model tests

Scale model tests of articulated vehicle stability have been performed with the remote-controlled test vehicle “Hjulus” (figure 22), developed at KTH within this project. The vehicle is an approximate 1:10 scale model of an articulated wheel loader, with a total length of about 100 cm and a mass of around 20 kg, depending on the load configuration. The vehicle uses an electromechanical steering system that uses coil spring to simulate the flexibility of a hydraulic steering system. The articulation angle is measured by a potentiometer and the vehicle is also equipped with accelerometers and gyros to allow the study of other vehicle dynamic states. The test vehicle is described in further detail in **Paper E**.



Figure 22: The scale model test vehicle "Hjulus", developed at KTH within this project.

In the basic setup, the vehicle has a fixed front axle and a freely pivoting rear axle, and is configured for all-wheel drive. Various combinations of mass and inertia properties have been analysed with respect to snaking and folding stability and are presented in greater detail in **Paper E**. Two examples of results are seen in figure 23. Here the vehicle has been subjected to a steering input while travelling in a straight line at a constant velocity of 1.5 m/s. Figure 23 (a) shows a case where the vehicle is in the original configuration, with no added weights. It is seen that the response is highly stable. Figure 23 (b) shows a case where extra weight has been added to the rear part. This rendered the rear yaw inertia higher in relation to the yaw inertia of the front part, resulting in an unstable configuration.

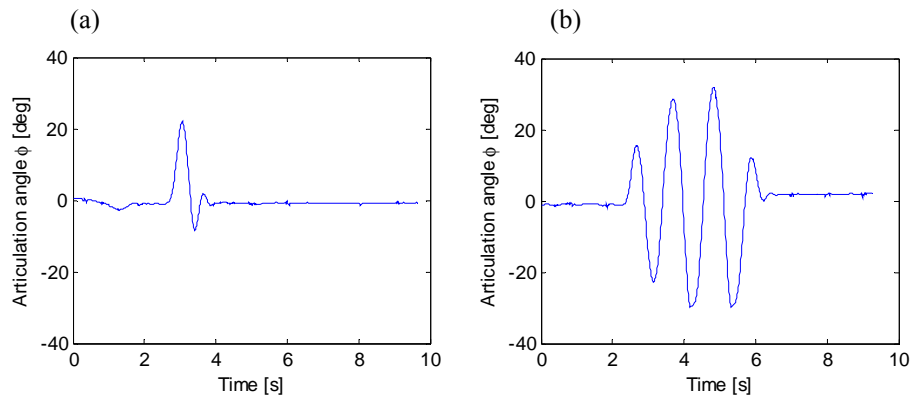


Figure 23: Test results for the scale model “Hjulus” in unsuspended configuration with (a) no extra masses and (b) with extra weight on rear part.

The corresponding stability predictions using the eigenvalue method are seen in figure 24. As seen in figure 24 (a), the original configuration is stable at the velocity considered (1.5 m/s), while the rear-heavy setup has an unstable snaking mode as shown in figure 24 (b). This is in agreement with the experimental results. Generally, it is found in **Paper E** that the linearised analysis is able to predict the stability properties of the vehicle with reasonable accuracy, although some tendency to under-predict the stability margins in comparison with the test results is noted. This is likely to be caused by various damping effects occurring in the model but not included in the linear analysis, such as the tyre aligning moment and the presence of friction in the centre joint.

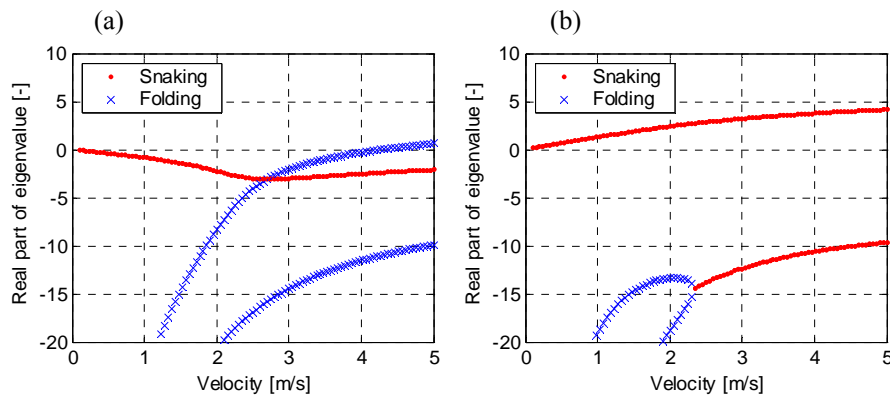


Figure 24: Eigenvalue analysis for the scale model vehicle, (a) in the original configuration and (b) with extra rear weights, showing folding (blue, crosses) and snaking (red, dots) eigenvalues.

### 3.4.1 Effects of the drive configuration

According to the linearised analysis, the drive forces do not affect the stability as long as the net yaw moment contribution is zero. This is the case with open differentials, where the left and right wheel torques are equal in magnitude (Azad, Khajepour and McPhee, 2007). The results from previously published multibody dynamic simulations are not unambiguous, as it has been stated by some authors that the longitudinal forces are small compared to the lateral forces and hence do not affect the snaking stability (Azad, Khajepour and McPhee, 2005b), whereas other studies on a roughly similar vehicle indicate that front-wheel drive results in improved lateral stability compared to all-wheel drive (Dudzinski and Skurjat, 2010). Hence, the influence of longitudinal forces warrants further investigation.

The influence of front- and rear-wheel drive has been investigated with the scale model vehicle by disconnecting the front or rear drive shafts, thus achieving a single-axis drive configuration. Results from these tests are shown in figure 25. The tests were performed at an initial velocity of 1.9 m/s and with added masses at the front and rear, to provide a response that is close to neutrally stable. Figure 25 (a) shows the results for the baseline vehicle with all-wheel drive, displaying a slowly divergent response at this velocity. Figure 25 (b) shows the response of the vehicle with front- and rear-wheel drive. It is seen that rear-wheel drive makes the vehicle unstable, as the articulation angle diverges quickly after the initial steering input. Interestingly, it can also be seen that front-wheel drive seems to result in deteriorated stability as well, although the response is different from that of the rear-wheel drive vehicle. Rather than experiencing the divergence seen in the rear-wheel drive case, the front-wheel driven vehicle enters a stable limit cycle after the initial disturbance.

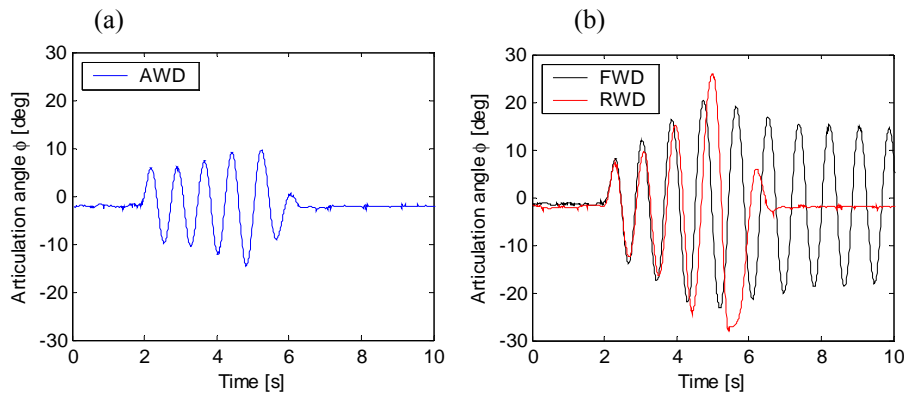


Figure 25: Experimental results with (a) all-wheel drive and (b) front-/rear-wheel drive.

It is clear from the results seen above that the driveline configuration influences the snaking oscillations of the vehicle. These experiments also show that linearised analysis is insufficient for lateral stability analysis when longitudinal forces are considered.

### 3.4.2 Effects of wheel suspension

The scale model vehicle can also be modified with various types of suspended wheel axles. This allows investigation of the influence of suspension on the snaking stability. Two suspension configurations have been analysed here. The first configuration includes independent front wheel suspension, using individual suspension arms and coil springs as the suspension elements. The rear axle pivots as in the baseline configuration, but with added rubber elements to provide roll stiffness. In the second configuration, individual suspension arms and steel coil springs are used for all the wheels, thus providing fully independent front and rear suspension. The roll frequency for both configurations is estimated to be about 6.0 Hz, based on tests with a stationary vehicle. The roll damping for the suspended vehicle is rather high, despite the low damping of the suspension springs. This is possibly due to high friction in the suspension linkages. Using data from stationary roll tests, the relative damping can be estimated to about 0.5, based on the time history of the lateral acceleration, which is measured above the roll centre. The two suspension setups show approximately the same damping rate.

The stability of the suspended vehicle is evaluated in the same way as that of the baseline configuration, initiating a steering disturbance when going straight at 1.9 m/s. The resulting responses can be seen in figure 26. All-wheel drive is used.

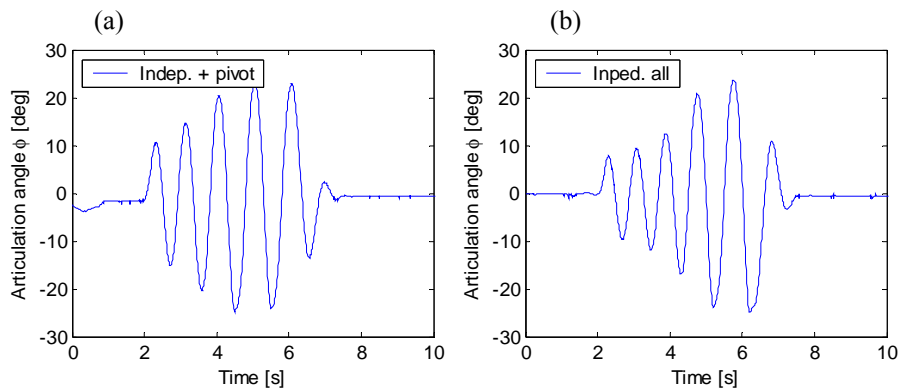


Figure 26: Vehicle response with (a) individual front suspension and (b) full individual suspension.

Comparing the results for the suspended vehicle to the baseline results in figure 25 (a), it is seen that both the suspended configurations display a slightly stronger divergence in the articulation angle, hence indicating a reduced stability margin. The frequency of the snaking oscillations is about 1.0 Hz for the suspended vehicle, as compared to about 1.3 Hz for the baseline vehicle. As in the multibody dynamics simulations (figure 20), it can be seen that the suspended mass roll seems to decrease the frequency of the snaking oscillations.

Generally, the results from the suspended vehicle seem to be in agreement with the multibody simulation results presented in **Paper D**: it is seen that suspended configurations display slightly decreased stability compared to the unsuspended

vehicle, but that the influence is less than that of other parameters such as mass, inertia and steering system properties. The responses of the two suspended configurations seem to be similar despite the differences in the suspension geometry. It should be noted that the modification of the wheel suspension removes about 0.5 kg of mass from each frame. As the changes are symmetric and close to the respective centres of gravity, the effect of these mass changes on the snaking stability should not be critical.

## 4. Effects of dynamic properties of large off-road tyres

With the exception of aerodynamic loads, any forces that affect a ground vehicle must be transmitted through the tyres. Hence, the dynamic response of the tyres will necessarily have a large influence on the dynamic behaviour of the full vehicle. Tyres for off-road use are designed to provide adequate traction on soft ground, and hence the tyres are large and have relatively low stiffness as compared to road vehicle tyres. This is partly an effect of low tyre pressure, as tests show that the traction is reduced considerably with increased tyre pressure (Noréus and Stensson Trigell, 2008). The low vertical stiffness leads to a nonlinear response and hysteresis due to large deflections. Furthermore, off-road tyres commonly face extreme durability demands that influence the structural design of the tyre, thereby implicitly affecting the tyre's dynamic behaviour. Construction machine tyres may also vary in design depending on the application, leading to considerable variation in the parameters.

The testing of large tyres is generally complicated and costly because of the size of the tyres, as well as due to the large forces required. Limited data is therefore available on off-road tyres in the sizes relevant to construction machines. Here a selection of published results is presented in order to illustrate the fundamental behaviour of various types of off-road tyres.

### 4.1 Related work on vertical properties

Vibration tests on non-rolling tyres have been published by Lehtonen et al (2006). A hydraulic test rig was used as the excitation source and three types of off-road tyres were investigated: a 14R20 military off-road tyre, a 710/45R26.5 forest machine tyre and a 16R25 heavy steel-belted tyre used by container handling vehicles and cranes. Compression tests showed that the quasistatic force-deflection behaviour was nearly linear, with the stiffness increasing with the tyre pressure. The tyre stiffness was largely independent of excitation frequency.

The vertical damping was estimated from the frequency response of the tyres. It was seen that the damping decreased considerably with increasing frequency, for all the tyres tested. One example is seen in figure 27, which depicts the damping of the military off-road tyre at two different inflation pressures: 4.5 bar (a) and 1.7 bar (b). Similar trends were observed for the other tyres. It can also be seen that the damping for this tyre has a peak at 1 Hz when inflated to 4.5 bar. This peak in the damping was not seen at a lower tyre pressure.

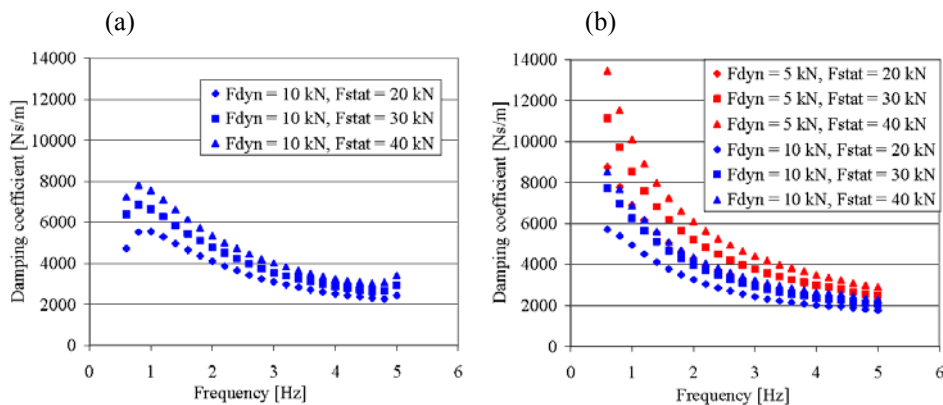


Figure 27: Damping for military off-road tyre at (a) a pressure of 4.5 bar and (b) a pressure of 1.7 bar (Lehtonen et al, 2006).

Besides the tendency of the damping to decrease with increasing frequency, the tyres also showed great variety in the magnitude of the damping. The forest machine tyre was seen to have a damping that was about three times higher than that of the military off-road tyre, resulting in higher relative damping at the load applied. The damping coefficient of the container handler tyre was comparable to that of the military tyre, although the stiffness was higher, which would result in lower relative damping at the tested load. Hence, tyres of comparable size but different structural design can be expected to exhibit different dynamic behaviour. The tyre damping was also affected by the dynamic and static loads applied, as indicated in figure 27.

Data on rolling agricultural tyres of the dimension 13.6R38 has been published by Lines and Murphy (1991a; 1991b), based on experiments using a trailing single wheel tester that is described in detail in an earlier report (Lines and Young, 1989). The tyre stiffness and damping were computed from the dynamic response when excited by a hydraulic shaker. The results (figure 28) show that the vertical stiffness, examined at 1.38 bar inflation pressure, was almost constant irrespective of the velocity and frequency. However, the static stiffness was typically 10-20% higher than the stiffness of the rolling tyre. It was also found that the stiffness increases with the tyre age due to rubber stiffening, but also that excessive wear of the tyre tread may decrease the stiffness because of less material in the lugs. Hence, the combined effect of old age and wear may be difficult to predict. Another noteworthy observation was that the tyre stiffness was independent of the applied driving torque.

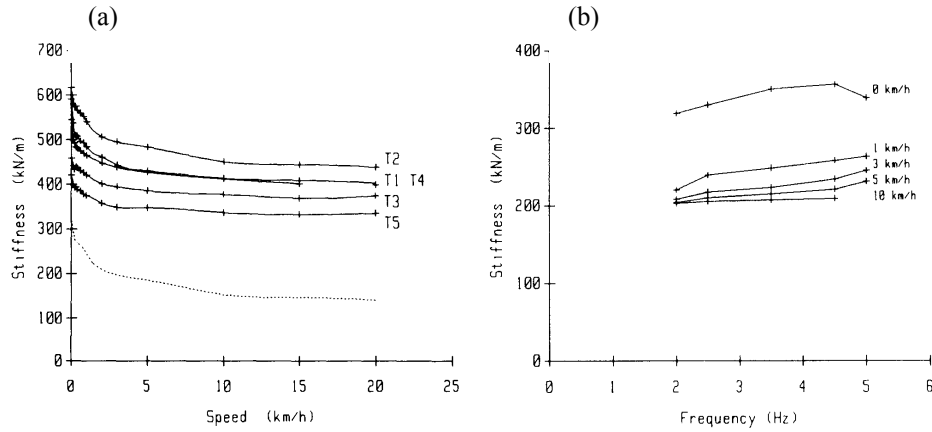


Figure 28: Influence of velocity (a) and frequency (b) on the stiffness of rolling agricultural tyres (Lines and Murphy, 1991a).

The damping of the rolling agricultural tyres, determined at 1.38 bar inflation pressure, was found to decrease with increasing excitation frequency and velocity in the same manner as the damping of the tyres tested by Lehtonen et al (2006), see figure 29. As in the case of stiffness, the damping is also higher for older tyres.

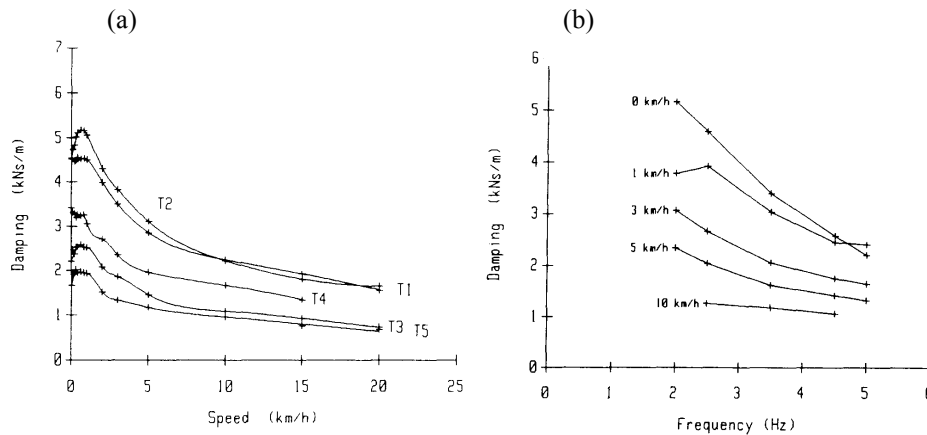


Figure 29: Influence of velocity (a) and frequency (b) on the damping of rolling agricultural tyres (Lines and Murphy, 1991b).

Tyre data from the measurements cited above have been used in ride vibration predictions using a multibody dynamics model on a corrugated wood track (Lines, Peachey and Collins, 1992). A point contact model was used for the tyre-to-ground interaction. Simulations with frequency- and velocity-dependent tyre properties proved more accurate with respect to the frequency response, but did not improve predictions of RMS accelerations. This indicates that the actual acceleration of the vehicle is also

dependent on local deformations of the tyre footprint. This could be an explanation as to why off-road ride predictions have historically been less successful (Crolla, 1981).

The combination of large radius and low speed also means that the radial run-out of off-road tyres may excite vibrations at relatively low frequencies. Tyre run-out is therefore important for large off-road tyres (Brinkmann and Schlotter, 2004). Tyre pattern excitation has also been seen to cause low frequency excitation in off-road tyres (Brinkmann and Schlotter, 2004). While pattern excitation mainly affects noise, it may be relevant to ride vibrations as well at low velocities, particularly when driving on hard surfaces.

## 4.2 Related work on lateral properties

The deformation of a tyre when subjected to an altered slip angle is not instantaneous, meaning that a time lag exists between a change in the slip angle and the resulting effect on the lateral force. This is true for any tyre, but is particularly relevant to off-road tyres, where the large size and flexibility can lead to considerable time delays in the lateral force build-up. Hence, the dynamic behaviour of lateral forces is different from the steady-state lateral response.

The lateral forces of an agricultural tyre of the dimension 16.9R34, inflated to 1.3 bar, have been investigated using a single wheel tester. Results from this test are cited by Schulze Zumkley and Böttinger (2009) and are seen in figure 30. The lateral force  $F_y$  is shown as a function of slip angle  $\alpha$ , plotted for different velocities ( $v_t$ ) and rates of change in the slip angle. The steady state force is also shown. It is clearly seen that the lateral force as a function of slip angle is lower when the slip angle is changing rapidly, indicating that the lateral force build-up exhibits a time delay. However, the effect is considerably less pronounced at the higher velocity. The static load was 10 kN.

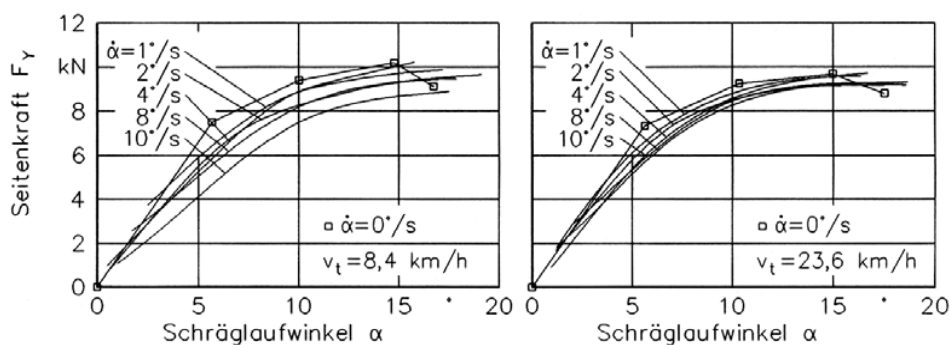


Figure 30: Lateral force (“Seitenkraft”) as a function of slip angle (“Schräglaufwinkel”) for agricultural tyres at varying velocity and rate of change in slip angle (Schulze Zumkley and Böttinger, 2009).

In general, the first order behaviour of the lateral force seen in figure 30 means that the vehicle will be less responsive to rapid steering inputs at low speeds. This is also relevant to the analysis of snaking stability, as discussed in Chapter 3. Since the lateral force develops slowly with rapid changes in the slip angles, increased snaking stability could be expected in some cases. However, the exact influence of this tyre behaviour may be more complex, since the lateral tyre forces are dependent on the frequency as well as the amplitude of the snaking oscillations.

### 4.3 Evaluation of a rolling test rig for large tyres

As a part of this research project, a rolling test rig for large tyres has been evaluated. The test rig consists of an unsuspended trailer designed to be towed by a heavy vehicle, as shown in figure 31. The test rig is instrumented with force transducers to measure tyre forces, as well as accelerometers and gyros for recording trailer motion. A detailed description is found in Appendix 1.



Figure 31: Rolling test rig for large tyres.

The test rig has been evaluated using a heavy road vehicle tyre (Goodyear Regional RHT, 385/65R22.5, inflated to 7.4 bar pressure), in order to provide a baseline for future off-road tyre measurements. The normalised frequency content of trailer vertical acceleration and roll rate, computed using a Fast Fourier transform (FFT), are shown in figure 32. It is seen that the bounce and roll dynamics of the trailer-tyre system are well defined, thus allowing analysis of the dynamic response of tyres without the disturbance of complex trailer dynamics.

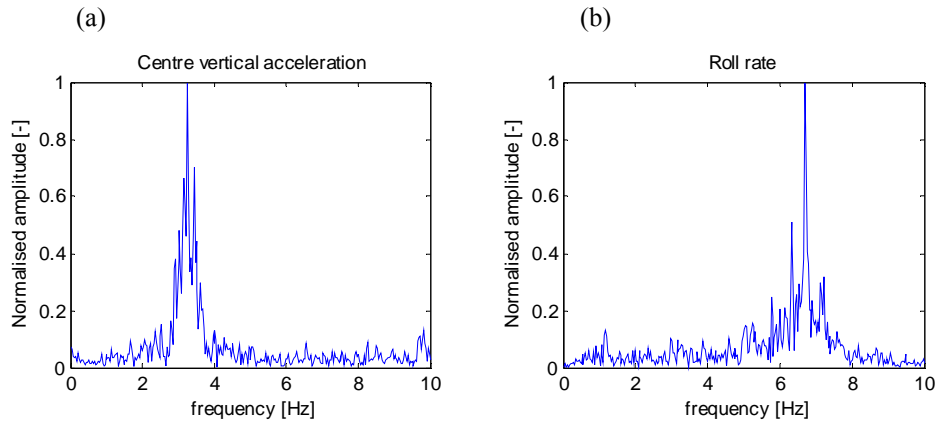


Figure 32: FFT of centre vertical acceleration (a) and roll rate (b).

Steady-state lateral data for the road vehicle tyre has also been gathered (figure 33), showing that the tyre is linear for small slip angles and that nonlinear behaviour starts above 4 degrees of slip angle. Hence, the rig is adequate for lateral measurements as well, although standard manoeuvres proved insufficient for creating large dynamic changes in slip angle. Figure 33 also shows a curve fit using the Magic Formula model (Blundell and Harty, 2004).

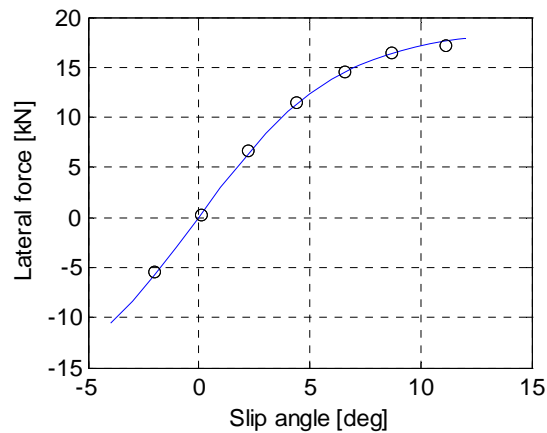


Figure 33: Steady state lateral force (-) and Magic Formula fit (o).

More information on this test rig is given in Appendix 1, including detailed descriptions of the signals recorded and the excitations used.

# 5. Multibody dynamics simulation and validation

Generally, a multibody system is any combination of rigid bodies connected by joints and/or flexible elements. Multibody dynamic simulations have become a common tool in the development of vehicles, since the method is well suited to describe the detailed mechanics of a ground vehicle and its subsystems, which typically consist of several rigid bodies and linkages. The oscillation of individual components may also be analysed in greater detail, which provides a more complete view of the higher order dynamics. This is particularly relevant to heavy vehicles, where ride vibrations may be affected by individual components (Gillespie, 1985). Dynamic events can also be recreated in detail in the simulation environment, thus providing an excitation that closely resembles an actual test.

## 5.1 Formalism and analysis modes

The basic function of multibody dynamics simulation software is to formulate the equations of motion for the dynamic system and integrate these over time to obtain the time history of system response. This is performed in different ways depending on the operation of the simulation software. Some applications derive the equations of motion symbolically, which allows the export of equations for use with external solvers or other software. Other programs use numerical formulations, which are usually integrated with the solver algorithm (Kortüm, 1993).

Integrating the equations of motion over time provides a dynamic analysis, which gives the resulting displacements and reactions as a function of the external forces that are applied. Another possibility is a static analysis, which finds an equilibrium position of the system. For vehicle dynamic applications, static analysis may sometimes be problematic since tyre models are not formulated to handle zero velocity, thus requiring modifications of the vehicle model in order to enable a static analysis. A linear analysis can also be performed, by linearising the equations of motion around an equilibrium position. The results from the linear analysis include natural frequencies and damping rates of the different vehicle eigenmodes. Linear analysis can provide elementary

validation information for a vehicle model if the relevant frequencies are known from testing. This approach has been used in **Paper A** as a tentative validation of an unsuspended wheel loader model.

An estimate of the complexity of a multibody system can be obtained from the number of degrees of freedom  $n_{DOF}$ , as computed by Gruebler's equation (Blundell and Harty, 2004):

$$n_{DOF} = 6 \cdot (n_{parts} - 1) - n_{const} \quad (29)$$

Here  $n_{parts}$  is the number of rigid parts in the model, including the ground, while  $n_{const}$  is the number of constrained degrees of freedom. The value of  $n_{const}$  therefore depends on the types of joints included in the model: a rotating joint without translation constrains all the degrees of freedom but one, hence  $n_{const} = 5$  for this joint; a spherical joint has  $n_{const} = 3$ . As an elementary example, a double pendulum can be considered. This system has  $n_{parts} = 3$  and  $n_{const} = 10$ , and thus two resulting degrees of freedom.

## 5.2 Model validation

Any simulation model requires validation if it is to be used for engineering purposes. An unvalidated or tentatively validated model may still be useful to predict trends or qualitative behaviour, but for predictions of actual response a validation process is necessary. For a multibody dynamics model, validation basically implies matching the response of the model to the measured response when the system studied is subjected to known excitations in the form of forces or displacements. As a vehicle is a large and complex dynamic system, it is usually not possible to validate every aspect of the dynamic behaviour, and the validation process therefore needs to be focused on the areas deemed most critical for the application of the model.

### 5.2.1 Subsystem validation

If possible, it is preferable to validate the subparts of the vehicle separately. For ride and handling analysis, the suspension and tyres can be considered the most important elements. Validation of suspension elements using test rigs has been demonstrated for leaf springs and hydraulic dampers (Anderson et al, 2001), as well as for suspension linkage kinematics (Rao, 2002). Validating suspension systems separately provides a possibility of defining suspension parameters with high accuracy, thereby enhancing the overall simulation fidelity. Subsystem testing may also reveal various nonlinear phenomena that are not obvious from full vehicle results. One example is friction in hydraulic suspension elements, which has been seen to influence suspension forces (Breytenbach, Cronjé and Els, 2010). In the case of interconnected suspension systems, such as a hydropneumatic suspension, it is also important that the layout of the test rigs should match the system layout when installed in the vehicle, since the details of the installation will affect the response of the total system.

Tyre dynamics is generally a source of uncertainty and it is therefore highly desirable to validate tyre models separately. This may be a problem for large tyres because of the need for large actuators and test rigs. Chapter 4 discusses some methods that have been used for the measurement of large tyre response. Appendix 1 also presents a test process for the dynamic behaviour of large tyres.

### 5.2.2 Whole vehicle validation

In full vehicle validation, the measured response of the vehicle is compared to the predictions from the simulation model. This requires a well-known excitation source, in the form of a surface profile or actuators. If no subsystem validation can be performed, it is usually not possible to isolate the influence of single parameters, as the whole vehicle response may be dependent on parameter combinations. An elementary example is the pitch or bounce frequency of the suspended mass, which is dependent on the suspension stiffness as well as on the mass and inertia of the vehicle body. Hence, exact values for parameters can not be determined from the full vehicle response alone and “reasonable” values may need to be accepted for the parameters involved. Sensitivity studies are also useful to reveal the relative influence of individual parameters on the full vehicle response. Optimisation methods have also been demonstrated for this purpose, in the validation of a multibody dynamics model of a passenger car (Rao, 2002).

As an additional measure to avoid uncertainties related to full vehicle testing, the validation scenario can be designed so that large loads and deflections are avoided, thus minimising the influence of the complex dynamics occurring in such excitations. The use of simple obstacles such as single bumps may reduce the local tyre deformations and shock loads on the suspension, something that could lead to discrepancies in linearised or otherwise simplified vehicle models. Good agreement with measurements has been seen in a model of an agricultural tractor traversing single, semicircular bumps (Lehtonen 2005). A similar validation has been shown for a heavy forestry vehicle (Hammarberg, Liukkula and Handroos, 1999). While validation against single obstacle excitations can show the basic validity of the model for small excitations, it does not guarantee accuracy when the vehicle is subjected to higher loads or more complex, three-dimensional forms of excitation.

The simulation accuracy can also be increased by determining the mass and inertia of the vehicle separately. While the mass and in-plane centre of gravity position can be easily found from weighing, determining the moments of inertia requires pendulum tests or similar testing methods, which may not be feasible for large vehicles. A modified approach using a spring-loaded rig has been demonstrated for an off-road passenger vehicle (Uys et al, 2006), providing reasonable accuracy with relatively low effort.

### 5.3 Multibody dynamics simulation of a suspended wheel loader

Presented here is an example of a full vehicle, multibody dynamics model. The model is based on a prototype wheel loader that has been modified with fully suspended front and rear axles. Both axles have been modified with three-point linkages and hydropneumatic suspension struts, which use bladder type hydraulic accumulators that function as constant mass gas springs. The total mass of the unloaded machine is 26,770 kg.

The simulation model has been created using the ADAMS multibody dynamics software (MSC Software, 2011) and is used in **Paper A** for ride comfort prediction. A graphic rendering of the model, with all included parts, is seen in figure 34. The coordinate system used is also seen here.

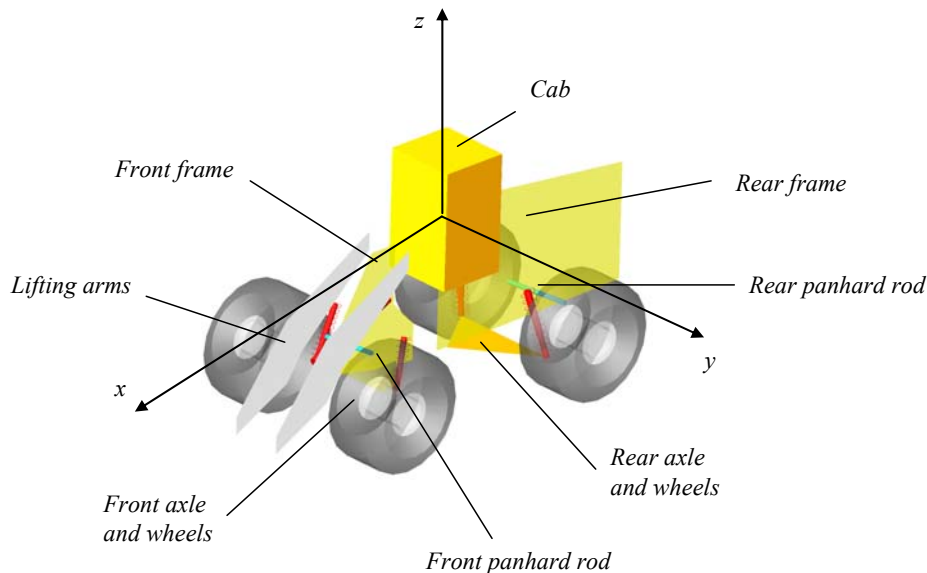


Figure 34: ADAMS model of a wheel loader with suspended axles.

The model consists of a total of 12 rigid parts, including the wheels, and has 22 degrees of freedom. The modelled three-point, rigid axle suspension linkage is based on that of the prototype vehicle, and includes Panhard rods for side forces. The main suspension springs are represented by linear spring and damper elements. The cab suspension elements of the actual machine consist of four oil-filled rubber elements mounted on the corners of the cab. In the simulation model, these are represented by bushings with linear stiffness and damping in three directions. The lifting hydraulics of the prototype machine are represented by a linear spring as well, to account for flexibility in the hydraulic system. The front and rear parts are connected by a revolute joint and the flexibility of the steering system is simulated by a torsional spring and damper element.

The tyres are described by the Fiala model (Blundell and Harty, 2004). This model represents the vertical tyre dynamics with a linear spring and damper element in combination with a point contact model.

### 5.3.1 Estimation of the vehicle and suspension parameters

The total mass and centre of gravity location of the whole vehicle have been determined through weighing. The mass and inertia of the individual parts have been estimated from the design specifications, and are adjusted so that the total mass matches that of the prototype machine. A summary of the fundamental parameters of the model is found in table 7. All the moments of inertia refer to the suspended mass.

Table 7: Parameters for the suspended wheel loader model.

Parameter	Value
Suspended mass	21,040 kg
Unsusended mass, total	5,730 kg
Roll moment of inertia	16,000 kgm <sup>2</sup>
Pitch moment of inertia	122,900 kgm <sup>2</sup>
Yaw moment of inertia	118,600 kgm <sup>2</sup>
Wheelbase	3.55 m
Centre of gravity position, suspended mass	1.68 m behind front axle, 1.31 m above ground
Centre of gravity position, total	1.69 m behind front axle, 1.22 m above ground
Dynamic pitch index	1.86
Front spring stiffness	412 kN/m
Rear spring stiffness	312 kN/m

The hydropneumatic suspension of the prototype loader is represented by linear springs in the simulation model. Since the pressure in the spring is sufficiently higher than the atmospheric pressure, the approximate linearised stiffness  $k_{cm}$  of the gas springs can be computed as (Harrison, 1983):

$$k_{cm} = \frac{\kappa N^2}{p_0 V_0} \quad (30)$$

where  $p_0$  and  $V_0$  are the preload pressure and the total volume of the accumulators in the hydropneumatic system, respectively. The load  $N$  on the spring is found from a static

analysis of the simulation model. The parameter  $\kappa$  is the polytropic index, which is assumed here to be 1.4, corresponding to an adiabatic compression and expansion of the gas volume. This approximation is deemed most suitable for the dynamic response of the suspension.

### 5.3.2 Comparison with measurements

To estimate the accuracy of the model described above, tests have been performed with the prototype wheel loader in unloaded condition. The vehicle was instrumented with two three-axis accelerometers on each axle and the suspension deflection was measured by four thread potentiometers mounted in parallel with the main suspension struts. Thus, the full motion of the axles and the suspended mass is captured. The cab is instrumented with a single three-axis accelerometer mounted at the seat console. All data was recorded at a sampling frequency of 160 Hz and filtered using a 20 Hz low pass filter, mainly to remove tyre pattern noise.

For excitation, the vehicle is driven over a ramp with a height of 0.13 m and a total length of 3 m, as seen in figure 35. The purpose of this obstacle is to provide an excitation that is mainly vertical, thereby avoiding deformations of the tyre belt in the longitudinal direction as much as possible since such effects complicate the response of the vehicle.

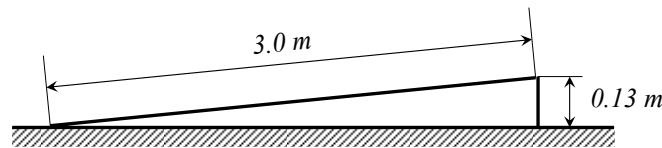


Figure 35: Ramp obstacle used as excitation.

The ramp was implemented in the simulation model as a two-dimensional input to the wheels. The tyre model used is a point follower type, meaning that the ramp edge would lead to unrealistic transients in the simulations. To remedy this, a simple smoothing of the surface profile was applied, so that the contact point would follow the actual path taken by a rigid wheel traversing the ramp.

Result sets are presented here for two different velocities, 5.1 m/s (18 km/h) and 8.8 m/s (32 km/h). The motion of the simulation model is controlled by individual torques applied at each wheel, controlled by a simple proportional controller. The simulated velocity was adjusted so that the time delay between the front and rear wheel excitations matches that seen in the measurements.

Figure 36 shows the measured and the simulated response of the left wheel vertical acceleration, at a velocity of 5.1 m/s. It can be seen that the model exits the ramp more abruptly than the real vehicle, despite the smoothing of the ramp profile used in the simulation. This leads to a larger initial transient in wheel acceleration. This also leads to a misalignment of the peaks in the time history, although the frequency of the resulting oscillations matches the measured frequency fairly well.

A low-frequency, lowly damped oscillation of relatively low amplitude can be seen after the initial transient. This is not adequately represented by the simulation model, where the initial motion instead is rapidly damped. Reducing the tyre damping of the simulation model does not affect this to any greater extent, since the axle bounce motion of the model is attenuated by suspension dampers as well as by tyre damping. It can also be seen that both the measured and the simulated accelerations are noticeably large in amplitude, reaching values in excess of  $30 \text{ m/s}^2$  at the front axle.

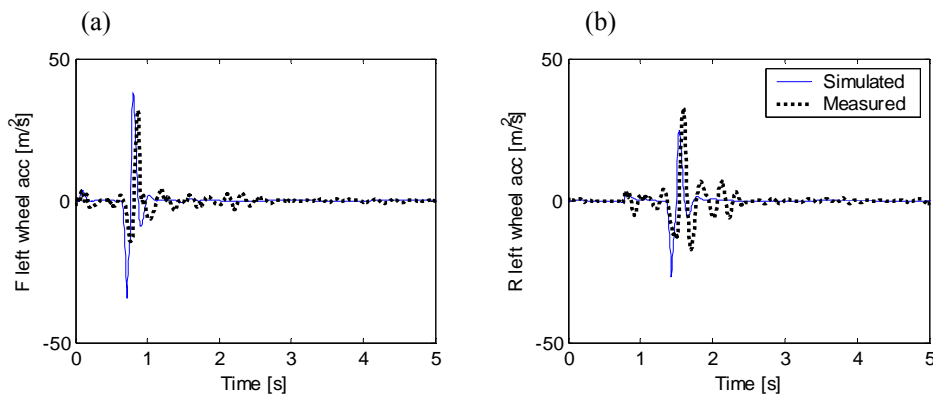


Figure 36: Results for left wheel vertical acceleration, front (a) and rear (b), evaluated at 5.1 m/s.

Figure 37 shows the simulated and the measured suspension deflection, with negative deflection signifying compression. Measurements are done at 5.1 m/s.

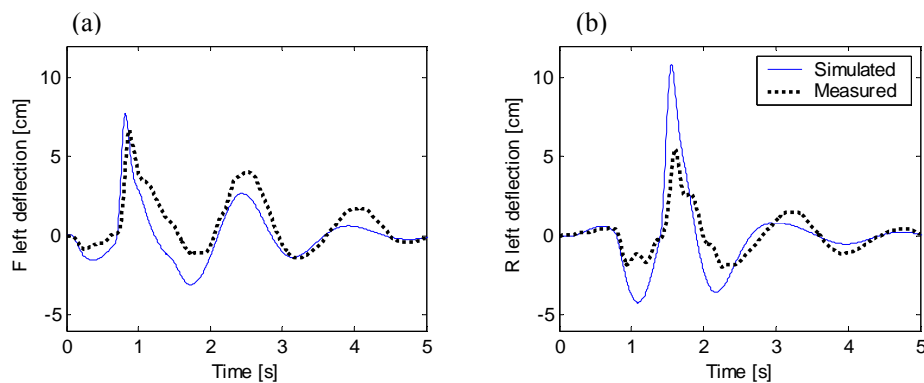


Figure 37: Results for left side suspension deflection, front (a) and rear (b), evaluated at 5.1 m/s.

The initial simulations indicated that the simulated motion with spring stiffness coefficients as in table 7 had too low a frequency, and the calculated spring stiffness was therefore increased 1.3 times to match the frequency of suspended mass oscillations. This results in the response seen in figure 37. The limits of the linear spring representation can also be seen here, since the measurements show that the deflections are larger in extension than in compression. This is to be expected, since gas springs are progressive in nature, increasing the stiffness with compression while

decreasing it with expansion. The simulated output instead shows a harmonic oscillation with roughly equal deflections in both directions. The initial transient seems to be over-predicted by the model for the rear suspension, but it is reasonably close to the measurement for the front suspension. This could possibly be related to nonlinear properties as well. A slight misalignment of the peaks can also be seen, as the initial excitation from rolling of the ramp occurs faster in the simulation model than in reality.

Figure 38 shows the front and rear wheel accelerations measured at 8.8 m/s. Compared to figure 36, the transient accelerations are only slightly larger despite the increased velocity. As in the case of 5.1 m/s, the front axle motion is more strongly damped. The transient accelerations are still exaggerated by the model, although the discrepancy is smaller than in the case with lower velocity.

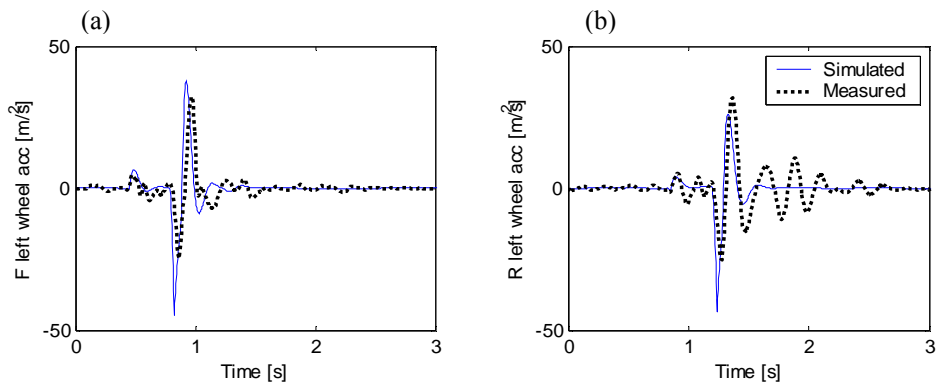


Figure 38: Results for left wheel vertical acceleration, front (a) and rear (b), evaluated at 8.8 m/s.

The suspension deflections at 8.8 m/s velocity can be seen in figure 39.

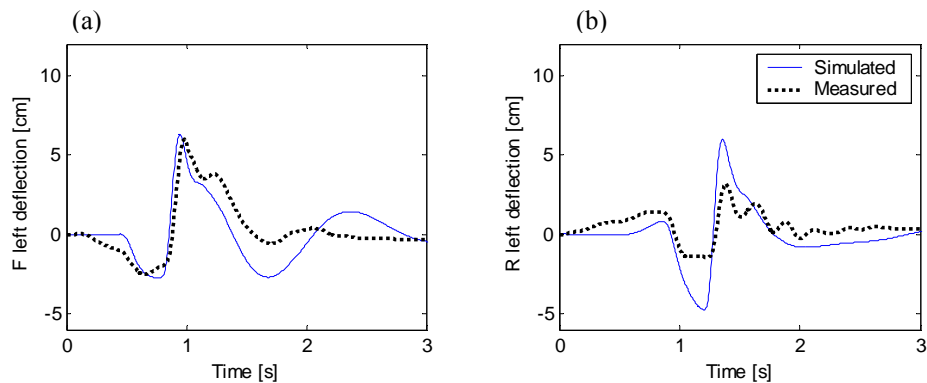


Figure 39: Results for left side suspension deflection, front (a) and rear (b), evaluated at 8.8 m/s.

Compared to the case with lower velocity (figure 37), the oscillations are considerably more strongly damped, which causes the simulation model to over-predict the suspension deflection. The frequency of motions is matched well although the different

shape of initial excitation makes it harder to compare the time histories directly. As for the wheel accelerations, this is caused by the inability of the simulation model to correctly emulate the ramp excitation.

The RMS vertical acceleration at the cab seat console is  $0.78 \text{ m/s}^2$  in the simulation and  $0.62 \text{ m/s}^2$  in the measurements, when measured at a velocity  $5.1 \text{ m/s}$ . The corresponding values at a velocity of  $8.8 \text{ m/s}$  are  $1.09 \text{ m/s}^2$  (simulated) and  $0.84 \text{ m/s}^2$  (measured). Hence, the model over-predicts the vertical acceleration by 25% to 30% in these cases. The time history of the simulated cab acceleration does not match the measured acceleration particularly well, indicating that a more refined model of the cab suspension is called for. As the cab mountings are small in dimension compared to other suspension elements, it should be feasible to define the response of these elements on the basis of rig testing.

### 5.3.3 General remarks

The comparison between simulated and measured response of the suspended wheel loader shows that the simulation model reasonably well matches the full vehicle when subjected to a simple excitation such as the ramp used here. Discrepancies mainly occur because of the point contact model used to represent the tyre-to-ground contact. Furthermore, local deformation in the tyre belt still seems to have an effect on the transient response of the axles, despite the simple excitation used. This is seen particularly in the wheel accelerations. Hence, it can be concluded that the tyre-to-ground contact is a critical point in modelling and will possibly have an implicit effect on the response of the suspended mass as well. One way to avoid this is to validate the suspended mass motion by using recorded axle motions as input to the simulation, thus neglecting the wheel and tyre dynamics. This approach has been demonstrated for the validation of a heavy truck model of high complexity (Anderson et al, 2001) and may increase the accuracy, since the uncertainty of tyre-to-ground interaction is removed, and also because the motion of the suspended mass can be validated separately from the unsuspended mass response. However, in the present case this would require the integration of accelerometer signals to provide axle positions, which leaves a number of problems related to the integration of low frequency accelerations.

The nonlinear characteristics of the suspension elements also affect the suspended mass motion. The inclusion of nonlinear suspension elements in the model would therefore be necessary for a more accurate simulation of the suspended mass dynamics. The presence of a suspended cab also represents a further complication, since the cab essentially adds a secondary suspended mass to the system. Hence, the degrees of freedom increase, although it should be feasible to obtain the parameters of the cab suspension from subsystem testing.



## 6. Summary and discussion of appended papers

### *Paper A: Ride comfort simulation of a wheel loader with suspended axles*

In this paper, a multibody dynamics simulation model is used to investigate how the addition of suspended axles influences the ride vibrations in a wheel loader. The suspension concept that is evaluated is a three-point, rigid-axle suspension with hydropneumatic springs. A model of an unsuspended wheel loader of the same size is used for comparison. The test case applied is a straight line traverse of a simulated test track, consisting of various symmetric and asymmetric bumps and depressions. RMS accelerations in the loader cab are used as a ride comfort measure, while the dynamic wheel loads and the vehicle roll angle are studied as indicators of the handling stability.

The simulation results indicate that the vertical and longitudinal accelerations of the suspended vehicle are reduced by a large amount compared to those of the unsuspended vehicle, but that the lateral accelerations are considerably less reduced, mainly because of the high roll stiffness. This is a general design conflict in off-road vehicles and does not seem to have a simple solution using passive components: decreasing the roll stiffness will reduce the handling stability of the vehicle and may therefore not be desirable, while lowering the placement of the driver seat would impair the driver's vision and therefore reduce productivity.

Due to the limited validation data, the simulation models used in the paper are simplified in many respects. The unsuspended wheel loader model is tuned to match the eigenfrequencies of an existing machine, but has not been validated with regard to transient response, which means that the results should be seen as comparative measures rather than absolute predictions. Nevertheless, the simulations indicate considerable improvements in ride vibrations and also identify the lateral direction as most critical. As this is in accordance with published studies on off-road vehicles (Els et al, 2007), it could be assumed that other predictions are at least qualitatively correct and may give a first estimate of the relative benefits of introducing a wheel suspension for this type of vehicle.

*Paper B: Pitch comfort optimisation of a front end loader using a hydropneumatic suspension*

The objective of this paper is to study how the pitching tendency of a wheel loader can be reduced, based on the well-known “flat ride” criterion (Best, 1984). This criterion implies that a stiffer rear suspension leads to decreased pitch response, usually at the expense of increased vertical accelerations. The flat ride suspension setup has been verified theoretically in a number of more recent publications, although it has been applied only to passenger cars. As the mass and inertia distribution of the wheel loader is different, this type of vehicle represents a different case. Furthermore, the suspension stiffness will change when loaded since the stiffness of the hydropneumatic springs increases with the applied force. As the vehicle carries the load ahead of the front axle, the front suspension will be considerably stiffer in the loaded configuration because of increased loading on the front axle. Likewise, the stiffness of the rear suspension decreases for the loaded vehicle. In this paper, frequency domain analysis, as well as multibody dynamic simulations, has been applied to investigate the effects of flat ride design on the dynamic behaviour of a wheel loader. The vehicle is studied in both the loaded and the unloaded configuration, taking into account the resulting changes in the suspension properties.

The results from linear analysis and simulations show that the pitch response of the unloaded vehicle is highly affected by the suspension setup, and that the pitch oscillations can be minimised with a moderate increase in the vertical acceleration if the rear suspension stiffness is sufficiently high. However, the possibilities for this may be limited in practice because of demands on static deflection as well as main ride frequencies. More importantly, the analysis shows that pitch oscillations may be reduced with a “reverse Olley” configuration as well, using stiffer springs on the front axle. This means that two optimal configurations could exist: one for the unloaded configuration and another for the laden vehicle, where the large increase in the front axle load leads to a stiffer front suspension.

While the design optimisation seen in this paper may not be feasible for all parameter combinations, it is clear that a stiffer rear suspension can reduce the pitch response for a wheel loader, despite the high pitch inertia. Thus, the “flat ride” design criterion, previously verified mainly for passenger cars, has here been successfully applied to a construction machine.

*Paper C: Influence of tyre properties on the ride dynamics of heavy off-road vehicles*

Construction machine tyres are large and relatively flexible compared to road vehicle tyres. This means that large deflections occur in the tyres and it can therefore be expected that tyre stiffness and damping will affect the response of the suspended mass. Moreover, the tyre parameters may vary widely because of the large diversity of operating environments. In this paper a linear half-vehicle model, including unsuspended mass dynamics, is used to analyse how the frequency response of a fully suspended wheel loader is affected by changes in the tyre properties. The resulting pitch and bounce accelerations when the vehicle is subjected to an ISO C-class surface (ISO, 1995) are used as ride quality indicators.

It is seen that the tyre stiffness and damping have a substantial influence on the RMS accelerations as well as on the main ride frequencies, and it is also seen that this influence is relatively independent of changes in the unsuspended mass. This indicates that the change in the suspended mass response is not caused by the oscillation of axles and wheels, but rather by the change in the combined flexibility of the tyre and main springs. Furthermore, it is seen that certain design tradeoffs are not affected by the tyre properties: the compromise between pitch and bounce acceleration, as well as the optimal damping for reduced ride vibration, is relatively unaffected by changing the tyre stiffness.

*Paper D: Snaking stability of articulated frame steer vehicles with axle suspension*

This paper analyses the lateral stability of an articulated wheel loader with regard to snaking oscillations. Similar studies have been conducted using planar analytical models, as well as multibody simulations, but none has included suspended mass roll motion in the analysis. The addition of a suspension to an articulated vehicle presents an additional degree of freedom that may affect the snaking stability, since the rolling motion of the suspended mass will interact with the snaking oscillations. A multibody dynamics simulation model of a wheel loader is used to investigate this. A simplified representation of the wheel suspension is used, allowing motion in roll only, with the equivalent torsion stiffness equal to the effective roll stiffness of the suspension springs.

From the simulation results, it can be concluded that suspension roll has a small detrimental effect on snaking stability, but that the influence is relatively minor compared to that of other parameters such as weight distribution or steering system properties. The greatest negative influence is seen when the suspension stiffness is chosen so that it leads to the natural frequency in roll coinciding with the snaking frequency. However, this effect is offset by small changes in the steering system properties or mass/inertia properties. Hence, it could be concluded that the addition of suspended axles is not critical for the snaking stability of articulated vehicles.

*Paper E: Scale model investigation of the snaking and folding stability of an articulated frame steer vehicle*

The main focus of this article is the development and testing of a remote-controlled, scale model vehicle for analysis of the lateral stability of articulated vehicles. The use of a scale model provides a cost-efficient and safe way of studying possibly unstable dynamics, if the results are representative for a full vehicle. In this study, a wheel loader model in an approximate 1:10 scale has been designed, built and evaluated in various configurations. A linearised analysis of the vehicle has also been performed, to evaluate the agreement between linear predictions and the tests.

The parametric studies presented in the paper are limited to alterations of the mass and inertia. Results from these tests show that the parameter influence is consistent with previously published results: the vehicle displays a less stable snaking behaviour when the rear mass and inertia are increased, whereas folding occurs more easily when additional masses are placed near the centre joint. It is also seen that the linear predictions agree reasonably well with the test results. Thus, the scale model can be

considered a useful tool for investigations of articulated vehicle stability. As the baseline setup can be altered in various ways, the influence of several other parameters on the snaking and folding stability can be examined. Two interesting areas are the effects of the drive configuration and suspended axles. Results from such studies have been included in Chapter 3.

## 7. Scientific contributions

The main scientific contributions of this thesis, as found in the appended papers and the introduction part, can be summarised as follows:

- An investigation, using multibody dynamic simulations, of how the addition of suspended axles affects the ride vibrations in a vehicle with layout and parameters typical for a medium size articulated wheel loader. Results indicate a substantial reduction of longitudinal and vertical vibrations, but also show that vibrations in the lateral direction are less affected unless the roll stiffness is reduced. This is presented in **Paper A**.
- The demonstration of “flat ride” suspension design applied to a wheel loader, showing with analytical results and simulations that the pitch oscillations of the loader can be reduced considerably by selecting sufficiently high rear suspension stiffness. Moreover, it is shown that it is possible to reduce pitch oscillations in the loaded condition as well by utilising the properties of the hydropneumatic suspension. The results are presented in **Paper B**.
- A theoretic analysis of how variations in the stiffness and damping of the tyres affect the dynamic response of a suspended wheel loader, as presented in **Paper C**. It is shown that the pitch and bounce accelerations of the suspended mass are significantly influenced by tyre properties, irrespective of changes to the unsuspended mass. However, design objectives such as minimised pitching are not affected by altered tyre characteristics to any greater extent.
- An investigation of how the rolling of the suspended mass influences the snaking stability of an articulated frame steer vehicle, using a multibody dynamics simulation model with a simplified suspension model allowing roll motion only. Simulations show that the suspended vehicle displays slightly deteriorated stability compared to a similar vehicle without suspension, but that the effect is small compared to that of other parameters such as mass distribution or steering system properties. This is presented in **Paper D**.
- An experimental study of the snaking and folding stability of articulated frame steer vehicles, using a scale model test vehicle. Results from driving tests are

compared to a linear analysis, showing that linear predictions estimate the stability properties with reasonable accuracy. The influence of mass and inertia on stability has also been investigated, reinforcing the results from previously published theoretical studies. These results are published in **Paper E**. The influence of suspended axles has also been analysed. Results are presented in section 3.4.1 and are in agreement with the simulation results from **Paper D**. The effects of driveline configuration on snaking stability is also investigated, showing that optimal stability is obtained with all-wheel-drive, as shown in section 3.4.2.

## 8. Conclusions and recommendations for future work

This thesis, including the appended papers, presents an overview of certain aspects of suspension design that are relevant to heavy off-road construction machinery. The findings presented are based on vehicle dynamic theory combined with simulations and empirical testing.

The analysis of ride dynamics shows that adequate pitch and bounce response can be attained with proper spring selection, and also that the pitch response of loader type vehicles can be attenuated, despite the high dynamic index. The relative damping is seen to decrease in loaded condition due to the increase in mass and inertia. This could possibly be overcome if suspension damping can be adjusted with load.

The greatest uncertainty for ride comfort improvement lies in the compromise between roll stability and reduced lateral acceleration. Simulations and past research indicate that passive systems have a limited capability to fulfil both requirements and it is therefore likely that active or semi-active systems are needed. While previous research has demonstrated that controlled damping or active roll control can improve the ride characteristics of off-road vehicles (Sarami, Meyer and Hammes, 2008; Cronjé and Els, 2009), this has still not been demonstrated for vehicles in the weight range of heavy wheel loaders or off-road dump trucks. Thus, preliminary studies of active roll control should focus on implementations of suitable control algorithms, as well as an investigation of the necessary energy requirements.

Investigations of lateral stability show that suspension roll does influence snaking and folding stability to some degree, but that this effect is less significant compared to the influence of mass distribution and steering system stiffness. This is confirmed by both multibody simulations and scale model tests. Furthermore, experiments with the scale model vehicle indicate that drive configuration may have a substantial impact on snaking stability. While this is not directly related to suspension design, it still warrants further investigation since the introduction of wheel suspension is likely to increase the transport velocities of articulated machines.

All the research work on articulated vehicle stability presented here has been concerned with open loop stability, without any corrective action from the driver or any other form of controller. As theoretical investigations (Horton and Crolla, 1986) as well as full vehicle tests (Lopatka and Muszynski, 2003) have indicated that driver-vehicle interaction may be the source of snaking oscillations, a possible area of future investigation could be the vehicle's lateral stability when acted on by a controller. Such a controller could be implemented as a driver model in simulation models, or by a combination of sensors and actuators in the scale model.

Various simulation models have been utilised in the present research work, as tools for preliminary investigations of suspension performance. The multibody dynamics simulation results of a suspended wheel loader correlate reasonably well with measured data from a real vehicle when excited by a single obstacle, although the accuracy of multibody simulation for vehicle response on three-dimensional uneven terrain has not been demonstrated. It is likely that the greatest uncertainty still lies in the tyre dynamics, and hence the generation of empirical tyre data is an area of great importance in the continued analysis of construction machine dynamics. The trailer tests reported on in Chapter 4 seems to provide a way to obtain data for vertical tyre properties as well as stationary lateral data. Rig tests possess a certain potential, but the sheer size of typical construction machine tyres could still make such testing unfeasible or overly expensive. Hence, methods that use the actual machine as a test rig should be examined, in order to test larger tyres.

While vehicle dynamic theory and simulations provide a starting point for suspension design, the continued development of construction machine suspensions will inevitably have to rely on experience from practical tests, using prototype machines. As construction machines are used in highly varying tasks and environments, field tests in realistic settings have the potential to provide a deeper understanding of stability and comfort that cannot be obtained using standard measures of ride and handling characteristics. The realisation of prototypes may also reveal practical limitations in the design space, and thereby narrow the range of available parameter combinations. Apart from prototypes and experimental machines, extended practical experience may also be gathered from tests with production machines, if the test scenarios are designed with ride and handling characteristics in mind.

On a general note, it seems obvious that the construction machine has evolved from merely being a self-propelled work machine to truly becoming a *vehicle*, with increasing demands on such properties as ride comfort and high-speed stability. This means that the requirements made on the vehicle dynamic behaviour of construction machines can be expected to increase in importance, existing in parallel with demands such as load capacity, tractive performance and durability. Vehicle dynamic theory and design methods, some of which have been demonstrated in this thesis, needs to be applied together with the growing base of knowledge obtained from continuous field testing and user experience. Applying this approach, a design paradigm for the construction machines of the future can emerge.

# References

- Anderson, D., Schade, G., Hamill, S., O’Heron, P. (2001), *Development of a multi-body dynamic model of a tractor-semitrailer for ride quality prediction*, SAE Technical Paper 2001-1-2764.
- Azad, N.L., McPhee, J., Khajepour, A. (2005a), *Tire forces and moments and on-road lateral stability of articulated steer vehicles*, SAE Technical Paper 2005-01-3597.
- Azad, N.L., Khajepour, A., McPhee, J. (2005b), *The effects of drive configuration on undesirable behaviours of articulated steer vehicles*. Paper presented at the 2005 IEEE Vehicle Power and Propulsion Conference, September 7, 2005, Dearborn MI, USA.
- Azad, N.L., Khajepour, A., McPhee, J. (2007), *Effects of locking differentials on the snaking behaviour of articulated steer vehicles*, Int. J. Vehicle Systems Modelling and Testing, Vol. 2, No. 2, pp. 101-127.
- Barak, P. (1991), *Magic numbers in design of suspensions for passenger cars*, SAE Technical Paper 911921.
- Best, A. (1984), *Vehicle ride – stages in comprehension*, Physics in Technology, Vol. 15, pp. 205-210.
- Blundell, M., Harty, D. (2004), *The multibody systems approach to vehicle dynamics*, Burlington: Butterworth-Heinemann.
- Bovenzi, M., Hulshof, C.T.J. (1998), *An updated review of epidemiologic studies on the relationship between exposure to whole-body vibration and low back pain*, Journal of Sound and Vibration, Vol. 215, No. 4, pp. 595-611.
- Breytenbach, B., Cronjé, P., Els, P.S. (2010), *The effects of suspension friction on off-road vehicle dynamics*. Paper presented at the joint 9th Asia-Pacific ISTVS Conference and Annual Meeting of Japanese Society for Terramechanics, September 27-30, 2010, Sapporo, Japan.
- Brinkmann, C., Schlotter, V. (2004), *High frequent excitation of agricultural tyres and the effect on driving comfort*. Paper presented at the joint 7th Asia-Pacific ISTVS Conference and 25th Annual Meeting of the Japanese Society for Terramechanics, September 11-16, 2004, Changchun, China.
- Cann, A., Salmoni, A., Vi, P., Eger, T. (2003), *An exploratory study of whole-body vibration exposure and dose while operating heavy equipment in the construction industry*, Applied Occupational Environmental Hygiene, Vol. 18, pp. 999-1005.
- Crolla, D.A. (1981), *Off-road vehicle dynamics*, Vehicle System Dynamics, Vol. 10, pp. 253-166.
- Crolla, D.A., Horton, D.N.L. (1983), *The steering behaviour of articulated body steer vehicles*, I. Mech. E. Conference Publications 1983-5, pp. 139-146.
- Cronjé, P.H., Els, P.S. (2010), *Improving off-road vehicle handling using an active anti-roll bar*, Journal of Terramechanics, Vol. 47, No. 3, pp. 179-189.

- Day, D.A. (1973), *Construction equipment guide*, New York: Wiley.
- Donati, P. (2002), *Survey of technical preventive measures to reduce whole-body vibration effects when designing mobile machinery*, Journal of Sound and Vibration, Vol. 253, No. 1, pp. 169-183.
- Dudzinski, P., Skurjat, A. (2010), *Probleme der Fahrstabilität von Radfahrzeugen mit Knicklenkung* (Motion stability problems in an articulated frame steering vehicle), ATZ Off Highway Special Edition, April.
- Dukkipati, R., Pang, J., Qatu, M.S., Sheng, G., Shuguang, Z. (2008), *Road vehicle dynamics*, Warrendale PA: SAE International.
- Els, P.S., Theron, N.J., Uys, P.E., Thoresson, M.J. (2007), *The ride comfort vs. handling compromise for off-road vehicles*, Journal of Terramechanics, Vol. 44, No. 4, pp. 303-317.
- Eriksson, P. (2001), *Optimisation of a bus body structure*, Heavy Vehicle Systems, International Journal of Vehicle Design, Vol. 8, No. 1, pp. 1-16.
- European Parliament (2002), *Directive 2002/44/EC of the European Parliament and of the Council, on the minimum health and safety requirements regarding the exposure of workers to the risks arising from physical agents (vibration)*, Official Journal of the European Communities, L 177:13.
- Fujimoto, Y. (1983), *Spectrum analysis of road roughness for earthmoving machinery*, Journal of Terramechanics, Vol. 20, No. 1, pp. 43-60.
- Gillespie, T.D. (1985), *Heavy truck ride*, SAE Technical Paper 850001.
- Gillespie, T.D. (1992), *Fundamentals of vehicle dynamics*, Warrendale, PA: SAE International.
- Gillespie, T.D., Karamihas, S.M. (2000), *Simplified models for truck dynamic response to road inputs*, Heavy Vehicle Systems, International Journal of Vehicle Design, Vol. 7, No. 1, pp. 52-63.
- Gorsich, D., Chaika, M., Sun, T.C. (2004), *Some statistical tests in the study of terrain modelling*, International Journal of Vehicle Design, Vol. 36, No. 2/3, pp. 132-148.
- Gransberg, D.D., Popescu, C.M., Ryan, R.C. (2006), *Construction equipment management for engineers, estimators, and owners*, Boca Raton, FL: CRC Taylor & Francis.
- Guo, Z., Fan, D., Xu, R., Tian, C. (2008), *Modal design optimization of an articulated frame*, SAE Technical Paper 2008-01-1589.
- Hammarberg, T., Liukkula, M., Handroos, H. (1999), *Simulation of the forwarder dynamics*, SAE Paper 1999-01-2783.
- Harrison, A.W. (1983), *Theoretical study of constant area gas springs in passenger car suspensions*, I Mech E Conference Publications 1983-5, pp. 97-106.
- Heydinger, G.J., Bixel, R.A., Garrot, W.R., Pyne, M., Howe, J.G., Guenther, D.A. (1999), *Measured vehicle inertial parameters – NHTSA's data through November 1998*, SAE Technical Paper 1999-91-1336.

- Holm, I.C. (1970), *Articulated, wheeled off-the-road vehicles*, Journal of Terramechanics, Vol. 7, No. 1, pp. 19-54.
- Horton, D.N.L., Crolla, D.A. (1986), *Theoretical analysis of the steering behaviour of articulated frame steer vehicles*, Vehicle System Dynamics, Vol. 15, pp. 211-234.
- International Organization for Standardization (1995), *Mechanical vibration - road surface profiles - reporting of data*, ISO standard 8608.
- International Organization for Standardization (1997), *Vibration and shock – evaluation of human exposure to whole-body vibration – Part 1: General requirements*, ISO standard 2631-1.
- Larsson, J., Broxvall, M., Saffiotti, A. (2005), *A navigation system for automated loaders in underground mines*. Paper presented at the 5th Int. Conf. on Field and Service Robotics (FSR-2005), 2005, July 29-31, Port Douglas, Australia.
- Lehtonen, T.J. (2005), *Validation of an agricultural tractor MBS model*, Int. J of Heavy Vehicle Systems, Vol. 12, No. 1, pp. 16-27.
- Lehtonen, T., Kaijalainen, O., Pirjola, H., Juhala, M. (2006), *Measuring stiffness and damping properties of heavy tyres*. Paper presented at FISITA World Conference, October 22-27, 2006, Yokohama, Japan.
- Lines, J.A., Young, N.A. (1989), *A machine for measuring the suspension characteristics of agricultural tyres*, Journal of Terramechanics, Vol. 26, No. 3/4, pp. 201-210.
- Lines, J.A., Murphy, K. (1991a), *The stiffness of agricultural tractor tyres*, Journal of Terramechanics, Vol. 28, No. 1, pp. 49-64.
- Lines, J.A., Murphy, K. (1991b), *The radial damping of agricultural tractor tyres*, Journal of Terramechanics, Vol. 28, No. 2/3, pp. 229-241.
- Lines, J.A., Peachey, R.O., Collins, T.S. (1992), *Predicting the ride vibration of an unsuspended tractor using the dynamic characteristics of rolling tyres*, Journal of Terramechanics, Vol. 29, No. 3, pp. 307-315.
- Lines, J., Stiles, M., Whyte, R. (1995), *Whole body vibration during tractor driving*, Journal of Low Frequency Noise & Vibration, Vol. 14, No. 2, pp. 87-104.
- Lopatka, M., Muszynski, T. (2003), *Research of high speed articulated wheel tool-carrier steering systems*. Paper presented at the 9th European Regional Conference of the ISTVS, September 8-11, 2003, Newport, United Kingdom.
- Milliken, W.F., Milliken, D.L. (2002), *Chassis design – principles and analysis*, Warrendale, PA: SAE International.
- MSC Software Corporation (2011), Official website, [www.mscsoftware.com](http://www.mscsoftware.com) [accessed 6/4/2011].
- Noréus, O., Stensson Trigell, A. (2008), *Measurement of terrain values and drawbar pull for six wheeled vehicle on sand*. Paper presented at the 16th international conference of the ISTVS, November 25-28, 2008, Turin, Italy.

- Olley, M. (1934), *Independent wheel suspension – its whys and wherefores*, Society of Automotive Engineers Journal, Vol. 34, No. 4, pp. 73-81.
- Rao, P.S. (2002), *Developing an ADAMS model of an automobile using test data*, SAE Technical Paper 2002-02-1567.
- Sarami, S., Meyer, H.J., Hammes, S. (2008), *Development and investigation of a semi-active suspension system for full suspension tractors*. Paper presented at the 16th international conference of the ISTVS, November 25-28, 2008, Turin, Italy.
- Sarata, S., Koyachi, N., Sugawara, K. (2008), *Field test of autonomous loading operation by wheel loader*. Paper presented at the 2008 IEEE/RSJ International Conference on Intelligent Robots and Systems, September 22-26, 2008, Nice, France.
- Schulze Zumkley, H.S., Böttinger, S. (2009), *Tyre parameter identification from road tests with agricultural tractors*. Paper presented at the 11th European Regional Conference of the ISTVS, October 5-8, 2009, Bremen, Germany.
- Segel, L. (1956), *Theoretical prediction and experimental substantiation of the response of the automobile to steering control*, Proceedings of the Institution of Mechanical Engineers, Automobile Division 1947-1970, Vol. 1956, pp. 310-330.
- Sharp, R.S., Pilbeam, C. (1993), *Achievability and value of passive suspension designs for minimum pitch response*. Paper presented at Vehicle Ride and Handling, international conference, November 5-17, 1993, Birmingham, UK. IMechE Conference Publications, 1993-9, pp. 243-259.
- Sharp, R.S. (2002), *Wheelbase filtering and automobile suspension tuning for minimizing motions in pitch*, Proceedings of the Institution of Mechanical Engineers, Part D: Journal of Automobile Engineering, Vol. 216, No. 12, pp. 933-946.
- Uys, P.E., Els, P.S., Thoresson, M.J. (2004), *Criteria for handling measurement*, Journal of Terramechanics, Vol. 43, pp. 43-67.
- Uys, P.E., Els, P.S., Thoresson, M.J., Voigt, K.G., Combrinck, W.C. (2006), *Experimental determination of moments of inertia for an off-road vehicle in a regular engineering laboratory*, The International Journal of Mechanical Engineering Education, Vol. 34, No. 4, pp. 291-314.

# Nomenclature

## Symbols

$A$	System matrix for planar articulated vehicle model
$A_p$	Effective area of gas spring piston
$C$	Damping matrix for pitch and bounce model
$c_1$	Front suspension damping coefficient
$c_2$	Rear suspension damping coefficient
$c_t$	Vertical damping coefficient of tyres, per axle
$C_i$	Cornering stiffness of tyre $i$
$C_{Mi}$	Aligning moment coefficient of tyre $i$
$C_R$	Equivalent torsion damping of articulated frame steering
$F_{y,i}$	Lateral force on tyre $i$
$F_z$	External force on pitch and bounce model
$G_d$	PSD of surface profile in spatial frequency domain
$G_w$	PSD of surface profile in temporal frequency domain
$G_{zz}$	PSD of suspended mass vertical acceleration
$G_{\theta\theta}$	PSD of suspended mass pitch acceleration
$H_{zw_1}$	Transfer function from $w_1$ to $z$
$H_{\theta w_1}$	Transfer function from $w_1$ to $\theta$
$I_{yy}$	Pitch inertia of suspended mass
$I_1$	Front part yaw inertia of articulated vehicle
$I_2$	Rear part yaw inertia of articulated vehicle
$K$	Stiffness matrix for pitch and bounce model
$K_R$	Equivalent torsion stiffness of articulated frame steering
$k_1$	Front suspension stiffness coefficient
$k_2$	Rear suspension stiffness coefficient
$k_{cm}$	Linearised spring stiffness of constant mass gas spring
$k_{cv}$	Linearised spring stiffness of constant volume gas spring
$k_t$	Vertical stiffness coefficient of tyres, per axle
$k_{tot}$	Sum of front and rear suspension stiffness

---

$L$	Wheelbase
$M$	Mass matrix for pitch and bounce model
$M_{z,i}$	Aligning moment on tyre $i$
$M_\theta$	External moment on pitch and bounce model
$m_1$	Front part mass of articulated vehicle
$m_2$	Rear part mass of articulated vehicle
$m_s$	Suspended mass
$m_{u1}$	Front unsuspended mass
$m_{u2}$	Rear unsuspended mass
$N$	Load acting on gas spring
$n$	Spatial frequency
$n_0$	Reference spatial frequency for ISO 8608 standardised surfaces
$n_{const}$	Number of constraints for arbitrary multibody system
$n_{dof}$	Number of degrees of freedom for arbitrary multibody system
$n_{gas}$	Molar gas quantity in gas spring
$n_{parts}$	Number of parts for arbitrary multibody system
$p_0$	Preload pressure for constant mass gas spring
$p_A$	Atmospheric pressure
$R$	Universal gas constant
$s$	Laplace variable
$T$	Absolute temperature of gas spring
$u$	Longitudinal velocity of articulated vehicle's front part
$V_0$	Accumulator volume for constant mass gas spring
$v$	Lateral velocity of articulated vehicle's front part
$v_x$	Longitudinal velocity
$W_1$	Laplace domain representation of $w_1$
$w_1$	Vertical surface displacement at front wheel
$w_2$	Vertical surface displacement at rear wheel
$x$	State vector for articulated vehicle model
$x_1$	Longitudinal position of articulated vehicle's front part
$y_1$	Lateral position of articulated vehicle's front part
$Z_s$	Laplace domain representation of $z$

$z$	Vertical displacement of suspended mass
$\alpha$	Lateral slip angle of tyre
$\zeta_z$	Relative damping in bounce
$\zeta_\theta$	Relative damping in pitch
$\Theta$	Laplace domain representation of $\theta$
$\theta$	Pitch angle displacement of suspended mass
$\kappa$	Polytropic index for ideal gas
$\lambda$	Longitudinal centre of gravity position, divided by wheelbase
$\tau$	Time delay between front and rear wheel excitation
$\varphi$	Articulation angle
$\psi_1$	Yaw angle of articulated vehicle, front part
$\psi_2$	Yaw angle of articulated vehicle, rear part
$\omega$	Angular frequency
$\omega_{0,z}$	Natural angular frequency in bounce
$\omega_{0,\theta}$	Natural angular frequency in pitch
$\dot{q}$	Time derivative of arbitrary variable $q$
$\ddot{q}$	Second time derivative of arbitrary variable $q$

## Abbreviations

AWD	All-wheel drive
DI	Dynamic index
DOF	Degrees of freedom
FFT	Fast Fourier Transform
FWD	Front-wheel drive
ISO	International Organization for Standardization
PSD	Power spectral density
RMS	Root mean square
RWD	Rear-wheel drive



# Appendix 1: Determining characteristics of large tyres by using full vehicle dynamic testing

## Background

In any vehicle dynamic analysis, the tyre is arguably the most complex dynamic element. This is especially true for large tyres, where the nonlinear response and hysteresis makes the behaviour of the tyres hard to predict. The size of the contact patch also leads to local deformations of the tyre belt, which affects the transmitted vibrations. Empirical testing of large tyres is complicated because of the large forces involved, and because of the size of the tyres. The only option is therefore often to estimate tyre data from tests with an actual vehicle, which adds considerably uncertainty since the vehicle and suspension dynamics influence the results. Static tests may only provide elementary insight since the characteristics of rolling tyres often differ from the stationary response.

This appendix describes a test method and an example of equipment for gathering the dynamic data that are of interest to determine the characteristics of large rolling tyres. An unsuspended rolling test rig, instrumented with force and motion sensors, is used to evaluate the response of the tyres on different surface profiles. The dynamic behaviour of the test rig itself is simple and well defined, thus allowing it to be used to determine the tyre properties without the disturbance of higher order dynamics. The surface profiles used as excitation have previously been profiled with high accuracy, thereby providing a repeatable and known input. Hence, measurement data can be used to validate tyre models of varying complexity.

## Methodology

### *Test equipment*

The main test equipment is a single axle, unsuspended trailer, seen in figure A1. The wheels are mounted rigidly to the vehicle frame, meaning that the entire trailer can be considered as a rigid body with reasonable accuracy. The lateral slip angle of each wheel hub can be fixed from minus -2 to about 12 degrees, in approximate steps of 2 degrees. Both wheels have a fixed camber angle of about 0.3 degrees, irrespective of the slip angle. This introduces a small bias error in lateral force.



Figure A1: The tyre test trailer with added weights.

The empty weight of the trailer is 4,705 kg, excluding wheels and tyres. Using a special frame and iron plates, as seen in figure A1, the total weight can be increased to about 10,000 kg. The trailer is designed to be towed by a heavy vehicle and the position of the hitch can be adjusted in fixed steps, so that the trailer is kept as level as possible for varying tyre dimensions. The mass and inertia of the unloaded trailer have been previously measured in lab tests. Static wheel loads are also measured before rolling tests.

### Measurements

Tyre forces are measured on the right hand tyre. This tyre is attached to a sub frame, which is connected to the main frame of the test trailer through load cells. Hence, all forces that are transmitted from the tyre to the trailer frame are recorded by the load cells. The test rig has six load cells in total: three in the vertical direction, two in the lateral direction and one in the longitudinal direction.

The lateral slip angle is measured with a Correvit S-CE optical sensor, mounted on a beam attached to the right wheel hub. Hence, the sensor gives the true slip angle of the tyre as it is always mounted in parallel with the rolling direction of the tyre. The trailer velocity is measured with optical sensors that record the angular velocity of each wheel hub. This provides an accurate estimate of trailer speed as long as wheel slip is close to zero, which is a reasonable assumption for free rolling tyres. Velocity is also measured by the Correvit sensor. Furthermore, a trailing “fifth wheel” is mounted on the rear of the trailer. The angular deflection of this wheel, measured by a potentiometer, gives an indication of the body slip of the test trailer.

For motion sensing, the trailer is equipped with a total of six accelerometers and three gyros, distributed as shown in figure A2. A three-axis accelerometer is located close to the centre of gravity, while vertical acceleration is measured in a point at the right side. Also, lateral and vertical accelerations are measured near the hitching point. The gyros are mounted on the front left side of the trailer. Since the trailer is considered a rigid body, angular velocities can be measured in any location on the main frame and the location used is chosen mainly for convenience. Figure A2 also shows the coordinate system used to define measurements. The  $z$  axis is perpendicular to the figure and positive upwards. The trailer is moving in the positive  $x$  direction.

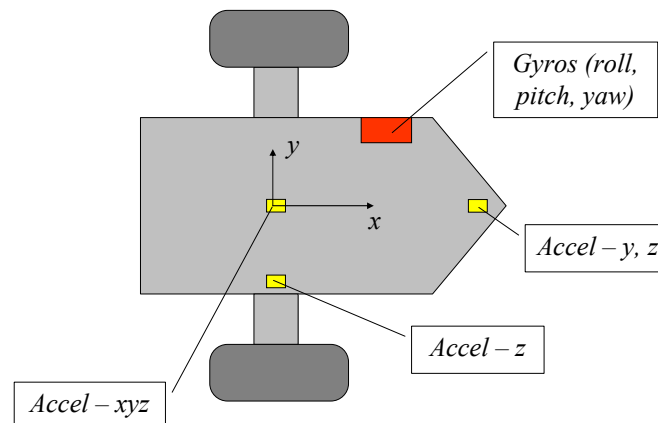


Figure A2: Location of accelerometers and gyros on the test trailer, top view.

A differential GPS antenna is also mounted on the towing vehicle, near the hitch. This provides an accurate measurement of the hitch position in the  $x$ - $y$  plane. Also, a video

camera is set up to record continuous images of the test track traversed by the right hand tyre of the trailer. By image processing, the exact path taken by the tested tyre can be recreated. This allows an accurate input to simulation models in combination with available surface profile data. A laser profilometer is also used to record a 2D profile of the test track.

All data is stored digitally with a sampling frequency of 1,000 Hz.

#### *Test tracks*

Testing is done on the Gerotek vehicle testing facilities outside Pretoria, South Africa. For tests of lateral force, a flat concrete track is used. For vertical tests, the following courses are utilised:

- *Single bumps*: these are iron obstacles with a trapezoidal shape, creating a single uncomplicated disturbance.
- *Belgian paving*: this consists of square blocks of about 20 cm size.
- *Random uneven track*: this track is a combination of relatively gentle undulations in three dimensions, providing a random excitation in both lateral and vertical directions. The maximum difference in surface height is about 10 cm.
- *Corrugations*: these are 2.5 cm high ridges set at even intervals of 20 cm, at straight angle or at about 20 degrees relative to the path of travel.

All the tracks used have previously been profiled in three dimensions using a mechanical device (Becker and Els, 2010) with a lateral resolution of 10 cm. Thus, the tracks provide a well known excitation for validation of simulation models.

#### *Test procedures*

When gathering steady state lateral data, equal slip angles are set for the left and right tyres. This gives a "toe-in" or "toe-out" configuration, which produces equal and opposite forces on the tyres, in theory resulting in zero body slip of the trailer. The towing vehicle is accelerated to the velocity corresponding to maximum engine rpm, and data is measured at constant velocity. To complement the steady state data, a single lane change manoeuvre is also performed at different velocities. This is done with zero slip angle set on the test rig.

For vertical data gathering, the trailer is towed over all test tracks detailed above. The towing vehicle is driven on a level surface to the side of the test track, so that oscillations of the hitching point are minimised. This is possible since the track width of the trailer is larger than that of the towing truck, as seen in figure A3.



Figure A3: Towing of the test trailer over Belgian paving track.

As in the lateral tests, vertical test are performed at different constant velocities, obtained by applying maximum throttle at different gears.

## Results

Using the procedures and equipment described above, measurements have been performed using a Goodyear Regional RHT heavy trailer tyre of dimension 385/65R22.5, inflated to 7.4 bar pressure (cold tyre). The unloaded diameter is 107 cm and the width is 39 cm. This particular tyre is designed for use on smooth roads and the pattern is relatively shallow. The dynamic behaviour of this tyre is therefore not representative for construction machine tyres, since the design of on-road tyres differ in important aspects from the tyres used by off-road machines. However, the tyre provides a useful baseline for evaluation of the test method and equipment, as the dynamics are unaffected by tyre pattern excitation or other types of excitation that may occur in more complex tyres.

### *Analysing the dynamic modes of the test trailer*

An indication of the fundamental oscillation modes of the trailer can be found from frequency analysis of the signals. These have been computed using a Fast Fourier Transform (FFT). Figure A4 shows the normalised FFT result of vertical acceleration, measured near the centre of gravity, and of the trailer roll rate. Distinct peaks can be seen at 3.2 Hz in bounce and at 6.7 Hz in roll. The measurements are analysed from measurements on a flat surface, which can be approximated as a low intensity random excitation of the trailer.

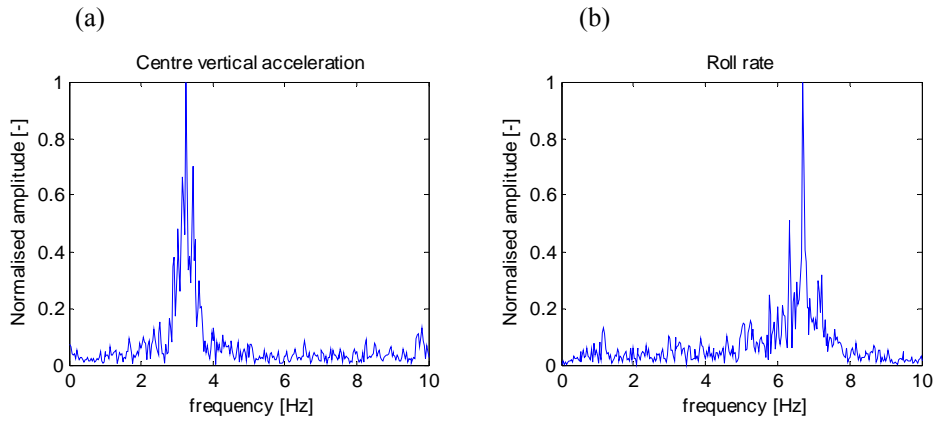


Figure A4: FFT of (a) centre vertical acceleration and (b) roll rate.

Figure A5 shows similar FFT results for trailer yaw rate and body slip, as measured by the trailing wheel. It can be seen that a resonance in yaw exists at 1.0 Hz, seen both in yaw rate and body slip. This yaw angle oscillation could not be observed during tests, and can therefore be assumed to be reasonably strongly damped.

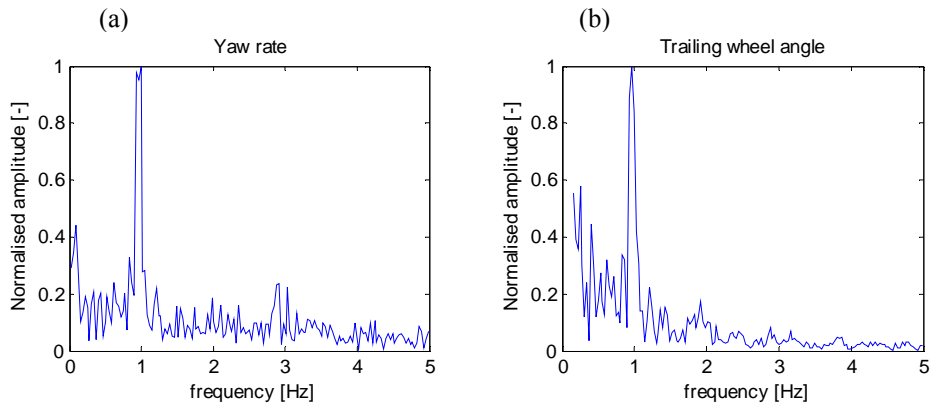


Figure A5: FFT of (a) yaw rate and (b) body slip angle.

From the frequency analysis of trailer motion, it can be concluded that the rigid body modes of the trailer are well defined and can be observed at distinct resonance frequencies. The dynamics of the test trailer can therefore be considered straightforward and uncomplicated, which allows focusing on tyre dynamics.

Steady state lateral force at different slip angles is computed by taking the mean value of slip angle and lateral force over a time interval where the velocity is constant. This is repeated for each discrete step in slip angle. The resulting force as a function of slip angle is shown in figure A6, together with an interpolation using the Magic Formula tyre model (Blundell and Harty, 2004).

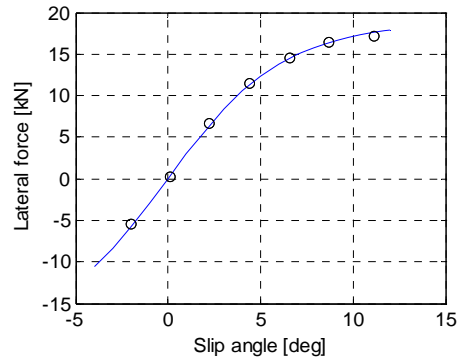


Figure A6: Steady state lateral force (o) and Magic Formula fit (-).

It is seen that the measurements provide adequate data in the linear range, from 0 to about 4 degrees slip angle. The nonlinear region is well described as well, although higher slip angles could be desirable to investigate since no distinct peak can be found in the available data. It can also be seen that the influence of camber force seems to be minimal as the measured force is small at slip angles close of zero degrees. Moreover, the stationary lateral force as a function of slip angle is well approximated by the Magic Formula curve.

The time history of the lateral force, shown in figure A7 for 6.5 degrees of slip angle, shows a distinct oscillation dominated by a 3.2 Hz mode corresponding to the trailer bounce resonance. From the time history (a), and from the normalised frequency spectrum of lateral force (b), it can be seen that the fluctuation of vertical force from trailer bouncing is affecting the cornering stiffness of the tyres, thereby causing an oscillating lateral force. It can also be noted that the trailer yaw oscillation at 1.0 Hz, as seen in figure A5, is not present in the frequency spectrum of the lateral force, implying that the trailer yaw oscillations does not affect the lateral slip angle of the tyre to any greater extent.

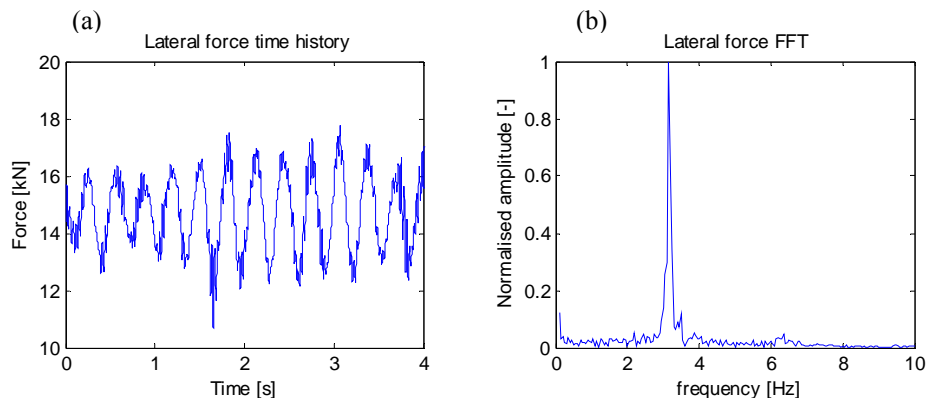


Figure A7: Time history (a) and frequency content (b) of lateral force, measured at 6.5 degrees lateral slip.

The time history of slip angle and lateral force from the single lane change manoeuvre are shown in figure A8. The manoeuvre has been performed at an initial velocity of 19 km/h and the data has been filtered through a 1.0 Hz low pass filter, for clarity. As the low frequency noise in the measured slip angle has about the same magnitude as the changes in slip angle during the manoeuvre, useful dynamic data can not be extracted from this measurement. Furthermore, comparing the lateral force plot in figure A8 (b) to the steady state data (figure A6) shows that slip angles during the manoeuvre are small, as the lateral force does not exceed 1.0 kN. It can also be seen that there is a 0.4 kN bias in the lateral force measurement, possibly because the manoeuvre was initiated in a slight turn. This could also be related to the presence of camber forces.

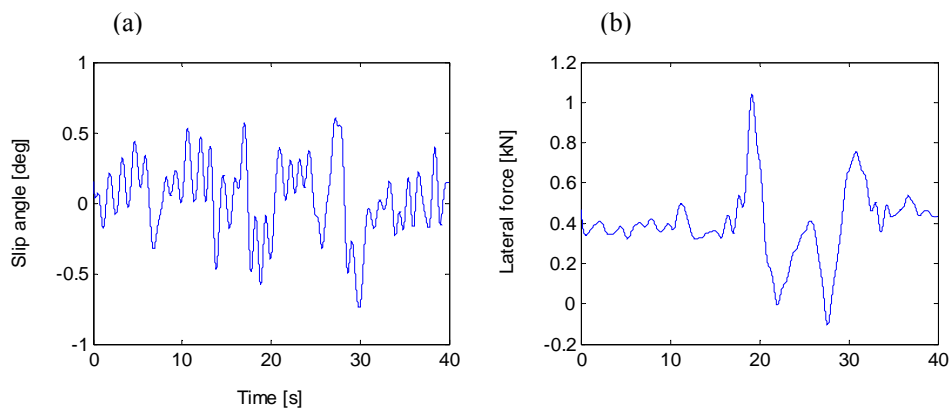


Figure A8: Slip angle (a) and lateral force (b), measured in a single lane change manoeuvre.

## Conclusions

From the frequency analysis, it can be seen that the trailer behaves like a simple unsuspended vehicle and that the rigid body modes are well defined. Frame bending or other effects are not visible in the frequency response of the trailer and tyre system. Hence, the dynamic response of the trailer is mainly determined by the tyre properties. This allows for stringent measuring of tyre characteristics.

It was observed that the vertical bouncing of the trailer is very lightly damped, even when running on level surfaces. The variation in vertical force caused by this bouncing is seen to have a relatively large influence on the lateral forces (figure A7 (a)), which may impair lateral force measurements. This could possibly be alleviated by a more refined hitch arrangement including friction dampers or similar, in order to dampen the trailer bouncing. Performing the measurements at low velocity also helps to alleviate the vertical oscillations of the trailer, although this was seen to result in higher noise in the slip angle when measured by the Correvit S-CE optical sensor. It could also be expected that trailer bouncing is less pronounced when evaluating low-pressure, off-road tyres, which generally have higher vertical damping than on-road tyres such as the one evaluated here.

The single lane change data proved insufficient for analysing dynamic changes in slip angle, as the slip angles developed during the manoeuvre are small and in the same range as the noise in the sensor. Since greater slip angles are difficult to get in by this manoeuvre, other means are necessary to provide a sweep in slip angle. The wheel hubs are prepared for hydraulic actuators, although these are currently not installed. If sufficient force can be generated, this would provide a powerful way to study effects of varying slip angle rate on lateral force. This is especially relevant for large off-road tyres, where considerable time lag in lateral force has been seen for rapid changes in slip angle (Schulze Zumkley and Böttinger, 2009). For construction machine tyres, the investigation of this effect is particularly important for the snaking and folding behaviour of articulated frame steered machines. Dynamic lateral data for off-road tyres, including the effects of rapidly changing lateral slip angle on lateral force, could provide considerably more accurate simulations of possibly unstable lateral modes.

Considerable tyre wear was noted after completed tests, caused by the thermal stress at large slip angles and high vertical load. This is likely to change the properties of the tyres over time. The effect of this is hard to quantify as it develops over time. One way of estimating errors caused by tyre wear is to perform several tests series over time, to provide a base for comparison.

## Future work

Primary data analysis from tests indicates that the test rig produces reliable and robust data. This means that it is possible to use trailer measurements to validate simulation models for large tyres. A multibody dynamics simulation model, seen in figure A9, has been developed for this purpose using the ADAMS simulation software (MSC Software, 2011). As the trailer is unsuspended and has no complicated dynamics, it can essentially be modelled as a rigid body.

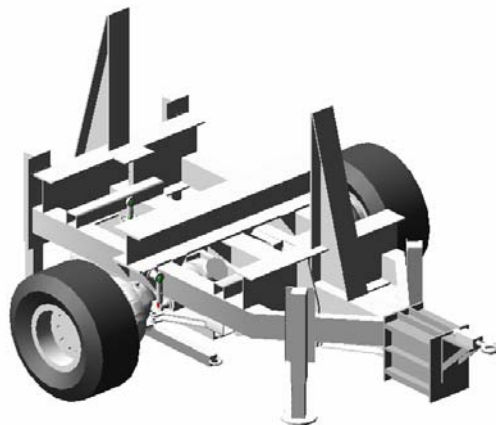


Figure A9: ADAMS model of the tyre test trailer.

For validation of lateral dynamics, the recorded GPS position of the hitching point can be used as input to the simulation model. This allows a direct comparison between measured and simulated tyre forces. The coefficients for the Magic Formula model can be obtained from the steady state tests, making implementation in ADAMS straightforward.

In vertical tests, the profiling data from the test tracks needs to be implemented in ADAMS as a three-dimensional road profile. Simulation of detailed tyre-surface interaction requires a model like FTIRE or similar (Gipser, 2007), to fully describe the local deformations of the tyre. In the case of FTIRE, additional static tests and modal analyses are necessary to parameterise the model. These can be performed in static rigs.

Rolling tests with smooth tyres show that the low frequency dynamics of the trailer are uncomplicated and well characterised by the rigid body modes. Thus, it is a suitable tool for testing off-road tyres as well, where complex dynamics such as tyre pattern excitation and vibration modes of the heavy tyre belt becomes important.

## References

- Becker, C., Els, P.S. (2010), *Profiling of rough terrain*. Paper presented at the Joint 9th Asia-Pacific ISTVS Conference and Annual Meeting of Japanese Society for Terramechanics, September 27-30, 2010, Sapporo, Japan.
- Blundell, M., Harty, D. (2004), *The multibody systems approach to vehicle dynamics*, Burlington: Butterworth-Heinemann.
- Gipser, M. (2007), *FTire – the tire simulation model for all applications related to vehicle dynamics*, Vehicle System Dynamics, Vol. 45, Supplement 1, pp. 139-151.
- MSC Software Corporation (2011), Official website, [www.mscsoftware.com](http://www.mscsoftware.com) [accessed 6/4/2011].
- Schulze Zumkley, H.S., Böttinger, S. (2009), *Tyre parameter identification from road tests with agricultural tractors*. Paper presented at the 11th European Regional Conference of the ISTVS, October 5-8, 2009, Bremen, Germany.